UNIVERSIDADE FEDERAL DO PARÁ
INSTITUTO DE CIÊNCIAS DA SAÚDE
PROGRAMA DE PÓS-GRADUAÇÃO EM CIÊNCIAS FARMACÊUTICAS

LEONARDO DE OLIVEIRA BITTENCOURT

A EXPOSIÇÃO PROLONGADA AO FLUORETO DURANTE A ADOLESCÊNCIA À FASE ADULTA MODULA O PROTEOMA HIPOCAMPAL E GERA DANOS COGNITIVOS ASSOCIADOS A UM PADRÃO NEURODEGENERATIVO NO HIPOCAMPO DE CAMUNDONGOS

BELÉM

2021

LEONARDO DE OLIVEIRA BITTENCOURT

A EXPOSIÇÃO PROLONGADA AO FLUORETO DURANTE A ADOLESCÊNCIA À FASE ADULTA MODULA O PROTEOMA HIPOCAMPAL E GERA DANOS COGNITIVOS ASSOCIADOS A UM PADRÃO NEURODEGENERATIVO NO HIPOCAMPO DE CAMUNDONGOS

Dissertação apresentada ao Programa de Pós-Graduação em Ciências Farmacêuticas da Universidade Federal do Pará, como requisito para obtenção do título de Mestre em Ciências Farmacêuticas.

Orientador: Prof. Dr. Rafael Rodrigues Lima

Coorientadora: Dra. Bruna Puty Silva Gomes

BELÉM

2021

Dados Internacionais de Catalogação na Publicação (CIP) de acordo com ISBD
Sistema de Bibliotecas da Universidade Federal do Pará
Gerada automaticamente pelo módulo Ficat, mediante os dados fornecidos pelo(a) autor(a)

B624e Bittencourt, Leonardo de Oliveira.
A exposição prolongada ao fluoreto durante a adolescência à fase adulta modula o proteoma hipocampal e gera danos cognitivos associados a um padrão neurodegenerativo no hipocampo de camundongos / Leonardo de Oliveira Bittencourt. — 2021.
87 f. : il. color.

Orientador(a): Prof. Dr. Rafael Rodrigues Lima
Coorientação: Profª. Dra. Bruna Puty Silva Gomes
Dissertação (Mestrado) - Universidade Federal do Pará, Instituto de Ciências da Saúde, Programa de Pós-Graduação em Ciências Farmacêuticas, Belém, 2021.

1. Flúor; Cognição; Fluorose; Neurotoxicidade; Proteômica.. I. Título.

CDD 615.90072

LEONARDO DE OLIVEIRA BITTENCOURT

A EXPOSIÇÃO PROLONGADA AO FLUORETO DURANTE A ADOLESCÊNCIA À FASE ADULTA MODULA O PROTEOMA HIPOCAMPAL E GERA DANOS COGNITIVOS ASSOCIADOS A UM PADRÃO NEURODEGENERATIVO NO HIPOCAMPO DE CAMUNDONGOS

Dissertação apresentada ao Programa de Pós-Graduação em Ciências Farmacêuticas da Universidade Federal do Pará, como requisito parcial para obtenção do título de Mestre em Ciências Farmacêuticas.

Aprovado em: 19/11/2021

Banca examinadora:

_____

Prof. Dr. Rafael Rodrigues Lima
Universidade Federal do Pará
Instituto de Ciências Biológicas

_____

Dra. Bruna Puty Silva Gomes
Universidade Federal do Pará
Instituto de Ciências da Saúde

_____

Profa. Dra. Ana Carolina Alves de Oliveira
Universidade Federal do Pará
Faculdade de Medicina de Altamira

_____

Profa. Dra. Juliana Silva Cassoli
Universidade Federal do Pará
Instituto de Ciências Biológicas

BELÉM

2021

AGRADECIMENTOS

À minha mãe, que sempre esteve ao meu lado vibrando pelas minhas conquistas e dando apoio aos meus projetos de vida; que é meu maior modelo de profissional da educação, que sempre incentivou e valorizou a minha formação acadêmica. Agradeço pelas cobranças por resultados dos seus investimentos em mim, sempre em dose certa, pelos aconselhamentos e ponderações sobre minhas escolhas, mas sempre me permitindo a ter minha autonomia e estendendo a mão quando precisei;

Ao meu pai e irmão, que sempre se importaram em saber sobre meus dias, passos e planos. Agradeço ao apoio que sempre me deram, por vibrarem pelas conquistas e sempre declararem o apoio às minhas escolhas enquanto profissional; Por sempre falarem comigo com boas doses de humor e leveza, por darem mais cor aos meus dias e sempre embarcarem junto comigo em meus projetos de vida;

Aos meus melhores amigos, Andrey e Andreia, pelo companheirismo e apoio de sempre. Agradeço por se importarem em saber como estava o desenvolvimento do meu trabalho, como eu estava de saúde e sempre declararem explicitamente a felicidade por cada conquista obtida; aos grandes amigos que o laboratório me deu, Iasmin Essashika, Leidiane Lima e Maria Olímpia, pelas companhias, momentos de lazer e boas conversas;

Ao meu incrível orientador, pelas oportunidades que me foram dadas, por acreditar no meu potencial e permitir me desenvolver para além de um futuro professor e pesquisador, mas como um ser humano mais sensível e ciente da realidade social que estou inserido; E à minha coorientadora, que desde a iniciação científica está presente em minha formação, estimulando a leitura de novos artigos, conversando sobre novas propostas de trabalho e me ensinando cada dia mais um pouco;

À equipe do Laboratório de Bioquímica na USP – Bauru, liderado pela profa. Marília Buzalaf, pela parceria na realização de experimentos e discussões científicas; Em especial às amigas e parceiras de pesquisa, Aline Dionizio e Tatiane Martini, por sempre me receberem tão bem e pela colaboração nos trabalhos que desenvolvemos;

À equipe do Laboratório da Farmacologia da Inflamação e Comportamento, em especial à profa. Cristiane Maia, por todo apoio técnico e científico na execução dos

testes comportamentais e por todos os trabalhos que são desenvolvidos através dessa parceria;

Aos meus colegas e amigos do laboratório que tornaram a rotina durante o mestrado sempre mais agradável. Agradeço especialmente à Maria Karolina pelo apoio durante a experimentação animal e coleta de amostras, e por ser uma amiga sempre disposta a estender a mão, e à Walessa Aragão, pela parceria nesse trabalho e amizade; agradeço também às amigas Victória Chemelo e Luciana Quirino pelo companheirismo, pelos cafés e risadas;

À Universidade Federal do Pará, pelo suporte financeiro e estrutural para a execução desse trabalho;

Ao CNPq, pela bolsa de mestrado a mim concedida durante o curso;

A Deus, pelas pessoas e oportunidades que me foram apresentadas nessa caminhada.

RESUMO

O fluoreto (F) é utilizado na fluoretação de águas devido à sua atividade anticariogênica e também está presente naturalmente e por ações antropogênicas em solos e reservatórios, caracterizando-se como um potencial poluente ambiental. Além da fluorose esquelética e dentária em pessoas que vivem em regiões com altos níveis de F, alguns estudos exploraram a associação entre a exposição ao F e danos cognitivos e, embora as evidências indiquem que apenas níveis elevados apresentam um efeito deletério sobre a cognição, um intenso debate tem crescido em relação à segurança da fluoretação artificial do abastecimento de água. Dessa forma, este estudo investigou se a exposição prolongada ao F, da adolescência à fase adulta, sob os paradigmas da fluoretação artificial do abastecimento doméstico de água e da questão ambiental, estaria associada a prejuízos de memória e aprendizagem em camundongos. Para isso, camundongos com 21 dias de idade receberam por 60 dias, 10 mg/L ou 50 mg/L de F na água de beber; o grupo controle recebeu apenas água sem adição de F. Em seguida, as funções cognitivas foram avaliadas pelo teste labirinto aquático de Morris e Esquiva Inibitória, seguido pela coleta de sangue e hipocampo para determinação do nível F plasmático e análise do proteoma hipocampal por espectrometria de massa. Alguns animais foram perfundidos para análises imunohistoquímicas da densidade de neurônios maduros nas regiões CA1, CA3, hilo e giro denteado (GD). Os resultados indicaram que a exposição prolongada ao F da adolescência à idade adulta aumentou a biodisponibilidade plasmática de F e a maior concentração de F desencadeou prejuízos de memória de curta e longa duração, estando associados à modulação do perfil proteômico global, além de um padrão neurodegenerativo nas regiões CA3 e GD. Assim, em uma perspectiva translacional, os achados dão evidências de potenciais alvos moleculares da neurotoxicidade do F no hipocampo, além de reforçarem a segurança de baixas concentrações de F e da necessidade de atenção às pessoas que vivem em regiões endêmicas.

Palavras-chave: Flúor; Cognição; Fluorose; Neurotoxicidade; Proteômica.

ABSTRACT

Fluoride (F) is used in artificial water fluoridation due to its anticariogenic activity, but it is also present in soils and natural reservoirs due natural high levels or anthropogenic actions, featuring it as a potential environment toxicant. In addition to skeletal and dental fluorosis in people living in regions with high F levels, some studies have explored the association between F exposure and cognitive damages, and although the evidences have indicated that only high levels pose a deleterious effect on cognition, a heated debated has grown regarding the safety of water supply artificial fluoridation. In this way, this study investigated whether long-term F exposure, from adolescence to adulthood, under the paradigms of water fluoridation and environmental issue, would be associated with memory and learning impairments in mice, and unravel molecular and morphological aspects involved. For this, 21-days-old mice received for 60 days, 10mg/L or 50mg/L of F in drinking water; the control group received only water without addition of F. Then, the cognitive functions were assessed by the Morris Water Maze and Inhibitory Step-down Avoidance test, followed blood and hippocampus collection for plasma F level determination, and hippocampal global proteomic profile analysis by Mass Spectrometry. Some animals were perfused for immunohistochemical analyses of mature neurons density in CA1, CA3, hilus and dentate gyrus (DG) regions. The results indicated that prolonged exposure to F from adolescence to adulthood increased plasma F bioavailability, and the higher F concentration triggered short- and long-term memory impairments, being associated with the modulation of the global proteomic profile, and a neurodegenerative pattern in the CA3 and DG regions. Our data, in a translational perspective, gives evidences of potential molecular targets of F neurotoxicity in the hippocampus and reinforces the safety of low fluoride concentration exposure, besides the need for attention of people living in endemic regions.

Keywords: Fluoride; Cognition; Fluorosis; Neurotoxicity; Proteomic.

SUMÁRIO

1. INTRODUÇÃO

O flúor é um elemento não-metálico pertencente ao grupo dos halogênios na tabela periódica e apresenta como principal característica química a sua alta eletronegatividade. Em seu estado elementar, o flúor é raramente encontrado na natureza, tendo a sua forma ionizada, o fluoreto (F^-), uma alta capacidade de formar compostos orgânicos e inorgânicos ao ligar-se com o hidrogênio, por exemplo, formando o ácido fluorídrico (HF), e ao sódio, formando fluoreto de sódio (NaF) (NCBI, 2021).

No meio ambiente, de forma natural, o fluoreto pode ser encontrado em minerais como fluorita (CaF_2), criolita (Na_3AlF_6), fluoroapatita [$Ca_5(PO_4)_3F$], e a villiaumita (NaF). Enquanto na indústria, vários compostos são sintetizados à base de fluoreto com as mais diversas finalidades, como os organofosforados sarin ($C_4H_{10}FO_2P$) e soman ($C_7H_{16}FO_2P$), na síntese química de fármacos, como a ofloxacina ($C_{18}H_{20}FN_3O_4$) e o 5-fluoruracil ($C_4H_3N_2FO_2$). O fluoreto também é utilizado na produção do hexafluoreto de urânio (UF_6) que é empregado no enriquecimento do urânio como combustível nuclear, na produção de gasolinas de alta octanagem, na alquilação de petróleo e de clorofluorcarbonos, que também são usados em aerossóis, refrigerantes e plásticos, por exemplo. Além disso, o fluoreto também é utilizado na fabricação do alumínio metálico, devido ao emprego da criolita (ALVARINHO et al., 2000; KIM et al., 2011; MUKHERJEE & SINGH, 2018).

O emprego do fluoreto na indústria do alumínio é bem consolidado, e vários estudos apontam altos níveis de fluoretos em trabalhadores, sujeitos à exposição ocupacional, níveis significativos no ar e em plantações aos arredores das indústrias. Diante disso, é evidente que o fluoreto é um potencial toxicante ambiental e ocupacional, especialmente quando não há utilização de adequada de equipamentos de proteção individual e manejo adequado dos rejeitos industriais. A exemplo disso, pode-se destacar o histórico da fluoretação da água de abastecimento doméstico com fins de promoção de saúde pública, devido às atividades anticariogênicas atribuídas ao fluoreto.

No início do século XX, Frederick McKay observou que crianças com manchas no esmalte dentário, futuramente denominadas de fluorose dentária, em Oakley (Idaho, Estados Unidos) apresentavam uma maior resistência dos dentes manchados ao desenvolvimento da doença cárie. Anos depois, na cidade de Bauxite (Arcansas,

Estados Unidos), McKay visitou a *Aluminum Company of America* (ALCOA) devido alguns relatos de fluorose dentária, constatando ao final que o quadro de manchamento do esmalte dentário era prevalente nas crianças da cidade de Buxita, mas não em outra cidade próxima. Os resultados dessa investigação chegaram à diretoria da ALCOA, quando o então químico H. V. Churchill resolveu avaliar a água potável da cidade e constatou altos níveis de fluoretos. Anos depois, em parceria com McKay, constataram que a resistência no desenvolvimento de doença cárie presente nas crianças de Oakley, estava associada à exposição contínua e à altas concentrações de fluoretos através da água potável de um poço (NARVAI, 2000; UNDE, PATIL & DASTOOR, 2018; ten CATE & BUZALAF, 2019).

A partir da descoberta, diversos estudos foram realizados a fim de elucidar os mecanismos envolvidos na atividade anticariogênica do fluoreto, assim como quais níveis poderiam ser considerados como eficazes e seguros às pessoas. Em 1945, portanto, os Estados Unidos e Canadá adotaram a adição de fluoretos à água de abastecimento doméstico como medida de saúde pública contra a doença cárie, ao mesmo tempo que serviram como estudos pilotos para avaliar a efetividade do método e posterior apresentação aos órgãos reguladores de segurança sanitária (NARVAI, 2000; AOUN et al., 2018). A primeira recomendação oficial da fluoretação artificial da água de abastecimento, em regiões desprovidas ou com baixos níveis de fluoreto, se deu pela *American Dental Association* em 1950, e depois oficialmente pela Organização Mundial de Saúde, que também passou a recomendar a incorporação de compostos fluoretados como o fluossilicato de sódio (Na_2SiF_6), ácido fluossilícico (H_2SiF_6), fluoreto de sódio e fluoreto de cálcio (NARVAI, 2000; AGNELLI, 2015; O'MULLANE et al., 2016). Essa recomendação também determina os níveis adequados, que atualmente estão entre 0,5 mg/L a 1,5 mg/L de fluoreto presente na água para consumo humano, podendo variar também até 1,7 mg/L devido às condições climáticas da região em questão, o que afeta diretamente o volume diário de água consumido. No Brasil, a fluoretação artificial do abastecimento doméstico foi oficialmente estabelecida pelo Governo Federal no ano de 1974, pela lei nº 6.050 24 de maio de 1974 e regulamentada pelo decreto nº 76.872, de 22 de dezembro de 1975 (NARVAI, 2000; RAMIRES & BUZALAF, 2007).

Entre as três maiores fontes de exposição ambiental ao fluoreto, ar, solos e água, os reservatórios subterrâneos de água são as maiores fontes (OMS, 2002), e o aumento dos níveis de fluoreto nos reservatórios está diretamente associado às ações

antropogênicas e naturais, como atividade industrial, despejo inadequado de rejeitos industriais, erosão de regiões com rochas com compostos fluoretados, que pode levar à infiltração do fluoreto em mananciais, lençóis freáticos e aquíferos subterrâneos. Um estudo de SANKHLA & KUMAR (2018) apontou que cidades da Índia apresentavam níveis de flúor que variavam de 0,03 a 16,9 mg/L; na China algumas regiões variavam entre 16 a 46 mg/L (CAO & LI, 1992). No Brasil, WHITFORD et al. (1999) reportaram que no estado da Paraíba os níveis de flúor variavam entre 0,1 mg/L a 2,3 mg/L, enquanto CORTES et al. (1996), mostraram que no estado do Ceará os níveis variavam de 2 a 3 mg/L. MOIMAZ et al. (2013) traçaram o perfil de fluoretação de águas em 40 cidades brasileiras durante 7 anos, e apontaram que cerca de 17% das amostras possuíam níveis acima de 0,84 mg/L, atingindo níveis de até 6,96 mg/L.

Os questionamentos a respeito do uso sistêmico, indiscriminado e/ou causado por exposição ambiental ao fluoreto ganharam reforços com o surgimento de evidências que o associam a danos em vários processos biológicos e diferentes órgãos, mostrando que diferentes concentrações de fluoreto, em diferentes tempos de exposição, são capazes de promover danos bioquímicos, genotóxicos, funcionais e/ou metabólicas (REDDY et al., 2014; BANALA et al., 2015; YAN et al., 2016), apresentando os efeitos deletérios mais prevalentes em humanos, causados pela exposição à altas concentrações de fluoretos, os quadros de fluorose dentária e esquelética (BUZALAF & LEVY, 2011; PECKHAM & AWOFESO, 2014).

Entretanto, muito além das desordens estruturais em tecidos mineralizados, estudos pré-clínicos apontam ainda que os efeitos deletérios do fluoreto estão associados ao desencadeamento de estresse oxidativo, déficit metabólico, neuroinflamação e morte celular por autofagia e apoptose (YANG et al., 2018; LOPES et al., 2020; SHUSHUA et al., 2021; LIMA et al., 2021; PUTY et al., 2021), tendo evidências que mostram danos sobre a glândula submandibular, testículos, tireoide e intestino e no sistema nervoso central (SNC) (JIANG et al., 2016; FENG et al., 2019; DIONIZIO et al., 2020; LIMA et al., 2021).

Em organismos adultos, a neurotoxicidade do fluoreto está associada a danos motores, emocionais e cognitivos em roedores (BARTOS et al., 2018; LOPES et al., 2020; CAO et al., 2021), sendo os danos de memória e aprendizado relacionados a modulações em componentes sinápticos, como *microtubule associated proteins* (MAP), sinaptofisina e receptores da via excitatória glutamatérgica, além de danos a componentes estruturais da bainha de mielina, como *proteolipid protein* (PLP) e

myelin-associated glycoprotein (MAG) (GE et al., 2018; NIU et al., 2018). Recentemente, o estudo de FERREIRA et al. (2021) apontou que exposição pré-natal ao fluoreto modula significativamente o perfil proteômico do hipocampo da prole, uma importante área envolvida em funções cognitivas, de ratos, além de aumentar a expressão de *brain derived neurotrophic fator* (BDNF) e gerar estresse oxidativo. Além disso, o estudo de DEC et al. (2019) mostrou que o fluoreto é capaz de desencadear um perfil pró-inflamatório no SNC.

Algumas evidências clínicas apontam que danos neurológicos relacionados às funções cognitivas podem estar associados a crianças expostas de modo dose-dependente, como apresentado por CHOI et al. (2012) e DUAN et al. (2018). Entretanto, em uma recente revisão sistemática e metanálise, (Miranda et al.2021) embora tenham ratificado a segurança da exposição à baixas concentrações de fluoreto, e que a exposição à altas concentrações estariam associadas a danos ao coeficiente de inteligência, os estudos observacionais disponíveis na literatura ainda carecem de robustez e qualidade no desenho metodológico, apresentando baixo nível de evidência.

Somado a isso, a literatura acerca dos mecanismos dos efeitos do fluoreto em processos cognitivos de memória e aprendizado ainda apresenta lacunas no entendimento, especialmente no que concerne ao SNC em desenvolvimento no período pós-natal, tornando oportuna a investigação de vias associadas a esses danos para maior compreensão e alerta aos possíveis riscos à saúde humana. Diante dessa problemática, esse trabalho objetivou investigar os efeitos da exposição a longo-prazo ao flúor em concentrações representativas da fluoretação de águas de abastecimento e de regiões endêmicas de fluorose, sobre aspectos bioquímicos e morfofuncionais de memória e aprendizagem associadas ao hipocampo de camundongos da adolescência à fase adulta.

A hipótese definida baseou-se na ratificação da segurança da exposição ao flúor em concentrações equivalentes à água de abastecimento, não gerando neurotoxicidade, observada a partir de aspectos bioquímicos, morfológicos e funcionais. Além disso, a segunda hipótese deste trabalho é que a exposição prolongada ao flúor em concentrações equivalentes às encontradas em regiões endêmicas de fluorose está associada a efeitos deletérios sobre funções cognitivas.

2. OBJETIVOS

2.1. OBJETIVO GERAL

Investigar se a exposição prolongada e sistêmica ao fluoreto, sob os paradigmas da fluoretação artificial do abastecimento doméstico e dos níveis encontrados em regiões endêmicas de fluorose, está associada à modulação de parâmetros moleculares, morfológicos e funcionais do hipocampo de camundongos jovens

2.2. OBJETIVOS ESPECÍFICOS

1) Avaliar possíveis mudanças na biodisponibilidade do fluoreto no plasma o de camundongos expostos a longo-prazo ao fluoreto;
2) Analisar a possível modulação do perfil proteômico hipocampal frente à exposição ao fluoreto durante 60 dias;
3) Avaliar se a exposição prolongada ao fluoreto causa danos às populações neuronais no hipocampo de camundongos;
4) Avaliar os possíveis efeitos da exposição prolongada ao fluoreto sobre funções cognitivas de aprendizagem, memória de curta-duração e memória longa-duração de camundongos expostos desde a adolescência à fase adulta.

3. ARTIGO CIENTÍFICO

3.1. CORPO DO ARTIGO

Long-term exposure to high concentrations of fluoride during adolescence to adulthood modulates hippocampal proteome and causes cognitive impairments associated with a neurodegenerative pattern in mice

Leonardo Oliveira Bittencourt[1], Aline Dionizio[2], Maria Karolina Martins Ferreira[1], Walessa Alana Bragança Aragão[1], Letícia Yoshitome[3], Sabrina de Carvalho Cartágenes[3], Luanna Melo Pereira Fernandes[3], Bruna Puty[1], Marília Afonso Rabelo Buzalaf[2], Cristiane do Socorro Ferraz Maia[3], Rafael Rodrigues Lima[1*].

[1]Laboratory of Functional and Structural Biology, Institute of Biological Sciences, Federal University of Pará, Belém, Pará, Brazil

[2]Department of Biological Sciences, Bauru Dental School, University of São Paulo, Bauru, São Paulo, Brazil

[3]Laboratory of Inflammation and Behavior Pharmacology, Faculty of Pharmacy, Institute of Health Sciences, Federal University of Pará, Belém, Pará, Brazil

***Corresponding author:**

Rafael Rodrigues Lima, PhD

Laboratory of Functional and Structural Biology, Nº 125, Institute of Biological Sciences, Federal University of Pará; Augusto Corrêa street n. 01, Guamá, Belém-Pará 66075-110, Brazil

E-mail: rafalima@ufpa.br

ABSTRACT

Fluoride (F) is used in artificial water fluoridation due to its anticariogenic activity, but it is also present in soils and natural reservoirs due natural high levels or anthropogenic actions, featuring it as a potential environment toxicant. In addition to skeletal and dental fluorosis in people living in regions with high F levels, some studies have explored the association between F exposure and cognitive damages, and although the evidences have indicated that only high levels pose a deleterious effect on cognition, a heated debated has grown regarding the safety of water supply artificial fluoridation. In this way, this study investigated whether long-term F exposure, from adolescence to adulthood, under the paradigms of water fluoridation and environmental issue, would be associated with memory and learning impairments in mice, and unravel molecular and morphological aspects involved. For this, 21-days-old mice received for 60 days, 10mg/L or 50mg/L of F in drinking water; the control group received only water without addition of F. Then, the cognitive functions were assessed by the Morris Water Maze and Inhibitory Step-down Avoidance test, followed by blood and hippocampus collection for plasma F level determination, and hippocampal global proteomic profile analysis by Mass Spectrometry. Some animals were perfused for immunohistochemical analyses of mature neurons density in CA1, CA3, hilus and dentate gyrus (DG) regions. The results indicated that prolonged exposure to F from adolescence to adulthood increased plasma F bioavailability, and triggered short- and long-term memory impairments, being associated with the modulation of the global proteomic profile, especially of proteins related to synaptic communication, and a neurodegenerative pattern in the CA3 and DG regions. Our data, in a translational perspective, gives evidences of potential molecular targets of F neurotoxicity in the hippocampus and reinforces the safety of low fluoride concentration exposure, besides the need for attention of people living in endemic regions.

Keywords: Fluoride; Cognition; Fluorosis; Neurotoxicity; Proteomic.

1. INTRODUCTION

Fluoride is a chemical element naturally found in the environment that has high electronegativity and a great capacity to form compounds by binding to other chemical elements, forming organic and inorganic compounds, such as hydrofluoric acid (HF) and sodium fluoride (NaF). In addition, fluoride is used in pharmaceutical industry, in the manufacture of aluminum, it is found in waste of ceramics production, burning of coal, and is also used in artificial fluoridation of water in the public domestic supply, due to its anticariogenic activity [1-3]

Since 1945, cities around the world fluoridate their public water supply [4] and the World Health Organization (WHO) determines optimal levels of fluoride that can be effective against caries disease, ensuring its safety and effectiveness, between 0.5 – 1.0 mg/L of fluoride [5], ranging from 0.7 – 1.2 mg/L depending on geographical conditions. Besides that, the WHO although recommends optimal fluoride levels, states that each local must consider others sources that would influence on daily intake [6]. However, several questions have been raised in history about safety and ethical issues involving artificially fluoridated water, which is often erroneously associated with high levels found in water for human consumption due to environmental pollution caused by industrial activity or even due to high natural levels, which may cause fluorosis and other possible neurological disorders [7,8].

Several observational studies have drawn an association between exposure to fluoride and its impacts on cognitive functions in developing organisms and adults, and there are also some systematic reviews and meta-analyses that suggest such association [9,10]. However, in a systematic review recently published by our group [11], we pointed out that the levels considered optimal by the WHO do not indicate an association with neurological disorders, but higher levels do, being associated with damages to the intelligence quotient. However, the strength of evidence available in the literature to date brings out the weakness of the assertion that any concentration of fluoride can be detrimental, contrasting with the robust evidence of the safety and effectiveness of low levels [12].

Thus, we used an experimental design to investigate the association of a low dose, considered representative of the artificial fluoridation of the domestic supply, and a high dose, representative of endemic regions of fluorosis, based on molecular, morphological and functional aspects in mice exposed from adolescence to adulthood

[13-17]. This window of exposure makes this investigation even more relevant due to the widespread knowledge that at this stage, the central nervous system is still under development, presenting similar human neurodevelopment events in children, adolescents, and young adults.

In this way, this research aimed to answer two main questions: Does prolonged exposure to low and/or high concentrations of fluoride trigger damages to memory and learning in mice? If only high concentrations do, what molecular and morphological characteristics are associated with the different pattern of response to the fluoride exposure? To answer that, we designed an experimental model using young animals and screened the global proteomic profile and hippocampus morphology that would be involved in the outcomes found, comparing the groups in a dose-response model perspective.

2. MATERIALS AND METHODS

2.1. BIOETHICAL ASPECTS

All the procedures were performed after ethics committee on the use of experimental animals' approval, under protocol nº 2422071217 CEUA-UFPA.

2.2. EXPERIMENTAL GROUPS AND EXPOSURE PROTOCOL

A total of 42 male mice (*Mus musculus*) with 21 days of age and body mass of approximately 10g were randomly divided into three groups of 14 animals each. The mice were housed in polypropylene collective cages (maximum of 5 animals per cage) and fed with food and water *ad libitum* inside a climate-controlled room, with a 12-hour light/dark cycle (lights on at 7 a.m.). For 60 days, the experimental groups received by voluntary consumption, *i.e.*, through a bottle, ultra-purified water with two different concentrations of fluoride (Sigma-Aldrich, USA), 10mg/L and 50mg/L, to mimic the chronic ingestion of F by humans in concentrations corresponding to ≅ 2 mg/L (equivalent to drinking water) and 10 mg/L (equivalent to water from areas endemic to fluorosis), respectively. These concentrations are justified by the need for fluoride administration to be 4 to 5 times higher in rodents, in order to reach plasma concentrations and clinical manifestations similar to those found in humans [18,19]. The control group received ultra-purified water without fluoride addition for the same period.

2.3. BEHAVIORAL ASSESSMENT

After the exposure period to fluoride, 14 animals from each group were randomly selected and taken to the behavioral testing room with attenuated sounds and controlled lighting and temperature. The animals' habituation to the environment occurred with a minimum period of 1 hour prior the beginning of the behavioral tests described below.

2.3.1. Step-down inhibitory avoidance test

The inhibitory avoidance test uses an aversive stimulus as a factor to obtain the behavioral response of short and long-term memories [20]. The protocol was based on Oliveira et al. [21], which was carried out in an acrylic box (50x50x35cm), with the bottom consisting of parallel stainless-steel bars, 1mm in diameter, connected to an electric current generator. Beside the metal bars, there is a “safe platform”, a region without spacing and not connected to the electrical stimulus generator. The test consisted of a 180 second habituation session, in which the animals were placed on the secure platform and the apparatus exploration was allowed. 30 minutes after the habituation, the animals were re-exposed to the secure platform with the face facing away from the observer and, immediately after the animal places all four paws on the steel bars, an electric shock of 0.4 mA was applied for 1 second (aversive stimulus). After 90 minutes of the aversive stimulus, the measure of short-term memory retention was evaluated in a test session, performing the same procedure of exposure to the apparatus, but without electrical stimulation and with a maximum latency of 180 seconds. The long-term memory test was performed 24 hours after the aversive stimulus, following the same exposure procedures without electrical stimulation and with a maximum latency of 180 seconds to observe the animal behavior. The times of training sessions and short and long-term tests were tabulated and expressed in seconds, comparing the groups with each other.

2.3.2. Water maze test

This test was used to assess the processes of learning and spatial memory according to the protocol described elsewhere [22,23] . The task consists of a circular pool filled with water (25°C) up to 30 cm, divided into four equal quadrants (Q1-Q4) and with a 29 cm high platform (10 cm²) made of blue acrylic was placed in the center of the target quadrant (Q4) for the training session and removed from the pool 24 hours

after training. The platform was camouflaged by adding non-toxic blue dye to the water; after that, each animal was submitted to four consecutive training sessions with an interval of five minutes each, period in which the animals remained on the platform for 20 seconds. If the animals were not able to find the hidden platform within 120 seconds, they were gently led to the platform, where they stayed for 20 seconds. The times in each quadrant and the time needed for the animals to find the platform were timed. On the test day (day two), animals were placed in the pool, in the absence of the platform, and allowed to explore the area for 60 seconds. In addition, the time needed to reach Q4, quadrant in which the platform was on the training day, and the time spent in Q4 were timed and plotted for statistical analyses.

2.4. SAMPLE COLLECTION PROCEDURES

A total of 18 animals (6 per group) was used for F plasma levels determination and proteomic analyses. Samples were collected after anesthetic induction with a solution of ketamine hydrochloride (90mg/kg) and xylazine hydrochloride (10 mg/kg) (i.p.), and after the loss of all foot and corneal reflexes, blood was collected through cardiac puncture with the aid of a 3mL syringe and heparinized tubes, with subsequent centrifugation at 3000 rpm for 10 minutes for plasma collection and freezing in a freezer at -20ºC. Afterwards, the brain was accessed for dissection of the hippocampal formation in ice-cold phosphate buffered saline (PBS). Afterwards, the samples were immediately frozen in liquid nitrogen and kept at -80 ºC.

2.5. FLUORIDE LEVELS ASSESSMENT

Prior the analysis, the removal of plasma CO_2 was performed by adding heated hexamethyldisiloxane (HMDS) [24,25]. Fluoride concentrations in the samples were determined in duplicate after HMDS-facilitated diffusion for 12h using the fluoride-specific electrode (Orion Research, Model 9409) and a miniature calomel electrode (Accumet, 13-620-79), both coupled to a potentiometer (Orion Research, Model EA 940). Standards of fluoride (0.0048 to 0.19 µg/mL) were prepared in triplicate and diffused in the same way as the samples. In addition, non-diffused standards were prepared to have exactly the same concentrations as the diffused standards. Millivoltage (mV) readings were converted to µg of F using Excel (Microsoft). A standard curve with a correlation coefficient of r=0.99 was established. Comparison of

mV readings will demonstrate that the fluoride in the diffused patterns has been completely extracted and analyzed (>95% recovery).

2.6. PROTEOMIC ANALYSIS

2.6.1. Protein Extraction and Digestion

In order to characterize the hippocampal proteomic profile of mice exposed to fluoride, the protocol was carried out following previous work by Bittencourt et al. [23,26]. Briefly, 6 samples from each group were pulverized individually by a cryogenic mill, with subsequent extraction of soluble proteins with lysis buffer [7M urea, 2M thiourea and 40mM dithiothreitol (DTT) in ammonium bicarbonate solution (AmBic, 50mM)] and recovered by centrifugating at 14,000 rpm for 30 minutes at 4ºC. Then, 100µg of protein from two samples, determined by Bradford's method [27], were pooled (becoming one single sample) and the following steps were performed in triplicate. A total of 50µg of protein was removed and diluted in AmBic 50mM to complete the 50µL volume with a concentration of 1µg/µL.

After protein extraction, the samples were alkylated and digested following the steps: 1) For each sample, 10µL of AmBic was added, followed by the incubation with 25µL of RapiGEST™ 0.2% (Waters Co., Manchester, UK) at 37°C for 30 minutes; 2) Then, 2.5µL of 100mM DTT were incubated at 37 °C for 60 minutes, followed by 2.5µL of 300mM iodoacetamide incubation for 30 minutes at room temperature (in the dark); 3) Afterwards, 10µL of trypsin was added and digestion occurred for 14 hours at 37 °C; Then, to interrupt the enzymatic action, 10µL of trifluoroacetic acid (TFA) 5% was incubated for 90 minutes with subsequent centrifugation at 14,000 rpm for 30 minutes. After that, the supernatant was collected and purified by Pierce C18 Spin column. At the end, the samples were taken to a vacuum concentrator where they reached the approximate volume of 1µL for subsequent addition of 5µL of Alcohol Dehydrogenase standard (1pmol/µL) + 85µL of acetonitrile at 3% for reading in the mass spectrometer.

2.6.2. Mass Spectrometry and Bioinformatics Analysis

The reading and identification of the peptides was performed in the nanoAcquity UPLC-Xevo QTof MS system (Waters, Manchester, UK). The difference in expression between groups was obtained using the ProteinLynx GlobarSERVER software, considering the level of statistical significance $p<0.05$ for down-regulated proteins and $1 - p>0.95$ for up-regulated proteins. The construction of the proteomic profile tables

was performed based on data from the Uniprot platform, through their accession IDs for comparison among the groups.

2.6.3. Bioinformatic Analyses

The bioinformatic analyses were conducted to define the functions from the Gene Ontology (GO) of biological processes, using the ClueGO plugin of Cytoscape v.3.7.2 software and protein-protein interaction networks were created by the ClustMarker plugin [28].

The over-representation analysis was performed as previously describe in Eiró et al., [29] and Ferreira et al., [15]. First, the data regarding the ratio of the previous analysis were processed and cut values were applied for screening proteins with expression value in 50% above or below in the exposed condition compared to the control. The analysis was performed considering only proteins with log2ratio values ≤ -0.58 or ≥ 0.58. Using the Uniprot conversion tool (https://www.uniprot.org/uploadlists/), the protein codes were converted into the record among gene IDs. For proteins with absolute changes, values were assigned -1 (for proteins detected only in the control) and 1 (for proteins detected only in the exposed sample). For the ORA analysis, the R studio program was used with the EGSEA plugin [30]. In this step, the Uniprot database was consulted, for the identification of proteins and the biological processes they participate in, made available by Bader Lab and after this verification we used the Cytoscape software [31] with Enrichment Pipeline plugin for grouping the sets of proteins previously consulted and after that the main biological processes were selected for graphic analysis. Subsequently, a protein-protein-interaction analysis was performed (https://www.networkanalyst.ca/) [32] to construct the representative image, according to the number of interactions of the proteins with the other proteins found altered. A minimum of 10 interactions was applied. The image was generated by the R studio program with the GOplot plugin.

2.7. MORPHOLOGICAL ANALYSIS

After the behavioral tests, 8 animals per group were randomly assigned to immunohistochemical evaluations, being firstly anesthetized with ketamine hydrochloride (90mg/kg) and xylazine hydrochloride (10 mg/kg) to be perfused with heparinized saline solution (0.9%) followed by phosphate buffered solution (0.2 M) of 4% paraformaldehyde. The brains were post-fixed in Bouin's solution for 4 hours, processed and embedded in Paraplast® (Sigma-Aldrich, USA) and cuts were obtained

at 5 µm in a microtome. For immunohistochemistry, the slides with sections were previously deparaffinized and immersed in PBS for 3 minutes before incubation in citrate buffer at 70°C for 25 minutes to recover the antigenic site. Then, to inhibit the endogenous peroxidase, the slides were incubated in a solution of methanol and hydrogen peroxide (3:100, v/v) for 30 minutes in the dark. We used the Anti-NeuN (1:100, Milipore) antibody, for quantitative investigation of neuronal populations after differentiation from neuroblasts to mature neurons and Horse anti-mouse secondary antibody (1:100, Vector Laboratories, USA). The revelation was performed by 3.3′ diaminobenzidine (DAB) in PBS, and mounted with coverslip and Entellan (Merck, Germany).

The NeuN+ cells counting was carried out in a bright field microscope (Nikon, eclipse E200) with a grid of 0.0062mm² coupled to the ocular lens, under 40x magnification. The hippocampal areas elected for cell count are CA1, CA3, Dentate Gyrus and Hilus, according to Bittencourt et al. [23]. The representative photomicrographs were taken by a DS-Fi3 microscope camera attached to the Nikon Eclipse Ci H550s bright field microscope.

2.8. STATISTICAL ANALYSES

Data were tabulated in GraphPad Prism 7.0 software. For data analyses, one-way or two-way ANOVA was performed depending on the variable, followed by Tukey's post-hoc test, assuming the value of $p<0.05$. The results were expressed as mean ± standard error of mean.

3. RESULTS

3.1. THE INCREASED FLUORIDE BIOAVAILABILITY DID NOT IMPACT ON BODY WEIGHT GAIN

The validation of the systemic administration was determined by fluoride plasma levels, and the results confirmed the exposure by the increasing fluoride bioavailability in a dose-dependent manner ($p = 0.0002$). The control group showed a mean concentration of 0.02 µg/mL (±0.002), while 10 mg/L group presented the concentration of 0.05 µg/mL (±0.007) and the 50 mg/L group, 0.08 µg/mL (±0.007) as shown in figure 1A. Moreover, the body weight gain during the experimental period was not affected by fluoride exposure ($p > 0.05$, Fig. 1B).

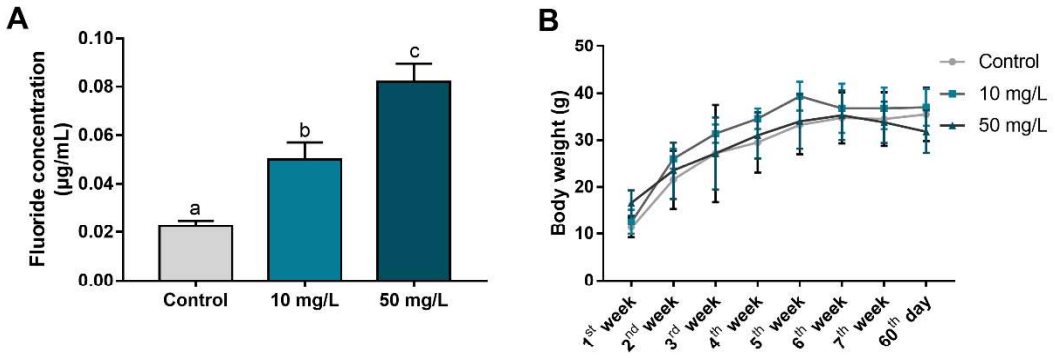

Figure 1. Effects of 60 days fluoride exposure to 10 mg/L or 50 mg/L from adolescence to adulthood on the fluoride plasma levels of mice (A) and body mass gain during the experimental period (B). Data are presented as mean ± S.E.M. In A, One-way ANOVA with Tukey's post-hoc test; In B, Two-way ANOVA with Tukey's post-hoc test. Different overwritten letters indicate statistical difference ($p<0.05$).

3.2. THE PROLONGED AND SYSTEMIC EXPOSURE TO F MODULATES THE GLOBAL PROTEOMIC PROFILE OF MICE HIPPOCAMPUS

The hippocampal proteomic profile of mice exposed to both fluoride concentrations were significantly changed according to the table 1.

Table 1. Quantitative distribution of proteins with different status of regulation among the group comparison

Comparison	Up-regulated	Down-regulated	Exclusive in first group	Exclusive in second group
10 mg/L vs. Control	126	65	136	117
50 mg/L vs. Control	121	23	140	104
50 mg/L vs. 10mg/L	86	138	109	87

The bioinformatic analysis of biological processes in which the proteins are involved showed a similar profile among the group comparisons as summarized in Table 2, being the most impacted processes related to morphological and energy metabolism aspects. The complete list of biological processes is presented on supplementary table 1 and the complete list of proteins of each comparison on supplementary tables 2, 3 and 4.

Table 2. List of biological processes based on Gene Ontology according to the hippocampal proteome in each group comparison

Group Comparison	**Biological Process**	**Number of genes (%)**
10mg/L x Control	Axon guidance	13.9
	Regulation of axonogenesis	12.6
	Dendritic spine morphogenesis	8.8

	Mitochondrial ATP synthesis coupled proton transport	7.5
	Glycolytic process through fructose-6-phosphate	6.3
	+ 16 biological processes	
50mg/L x Control	Axon guidance	13.5
	Regulation of axonogenesis	10.6
	Mitochondrial ATP synthesis coupled proton transport	6.7
	Regulation of dendritic spine development	6.7
	Transcription corepressor activity	5.8
	+ 22 biological processes	
50mg/L x 10mg/L	Regulation of axonogenesis	12.6
	Axon guidance	9.5
	Positive regulation of dendritic spine development	9.5
	Arp2/3 complex-mediated actin nucleation	7.4
	Mitochondrial ATP synthesis coupled proton transport	6.3
	+ 20 biological processes	

The over-representation analysis (Figure 2) showed the interaction of 59 proteins categorized in six main biological processes according to Gene Ontology, as cellular component organization, nervous system development, response to stimulus, metabolic process, nervous system process, synaptic signaling.

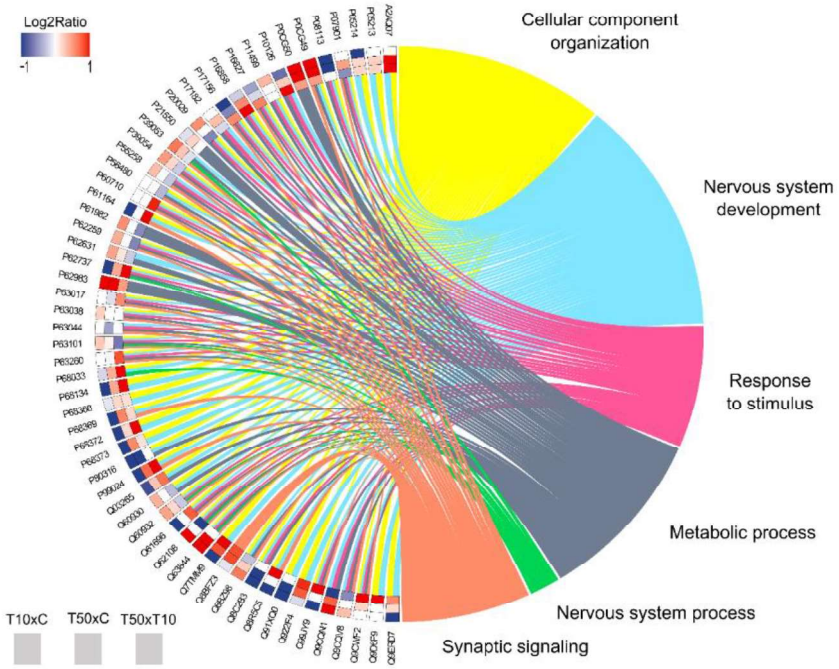

Figure 2. Circos plot chart of protein-protein interaction (PPI) in the hippocampus of mice exposed to 10mg/L or 50mg/L of fluoride. The PPI are associated with biological processes as cellular component organization (yellow), nervous system development (light blue), response to stimulus (pink), metabolic process (greyish blue), nervous system process (green) and synaptic signaling (beige), based on Gene Ontology annotations. Each protein is described with its respective Uniprot accession ID, and each colorful rectangle indicate a different comparison, with log2ratio ranging from -1 to 1.

3.3. THE LONG-TERM F EXPOSURE CAUSED A NEURODEGENERATIVE PATTERN IN HIPPOCAMPUS OF MICE ONLY IN THE HIGHEST CONCENTRATION

The exposure to 50 mg/L of fluoride during 60 days reduced the mature neurons density in CA3 when compare to control and 10 mg/L groups (adj. p value < 0.0001), and in Dentate Gyrus, when compared to control group (adj. p value = 0.02). No significant changes were observed in CA1 and hilus regions (p>0.05; Fig. 3) in 50 mg/L exposed group, and no difference was diagnosed in any hippocampal area of animals from 10 mg/L group.

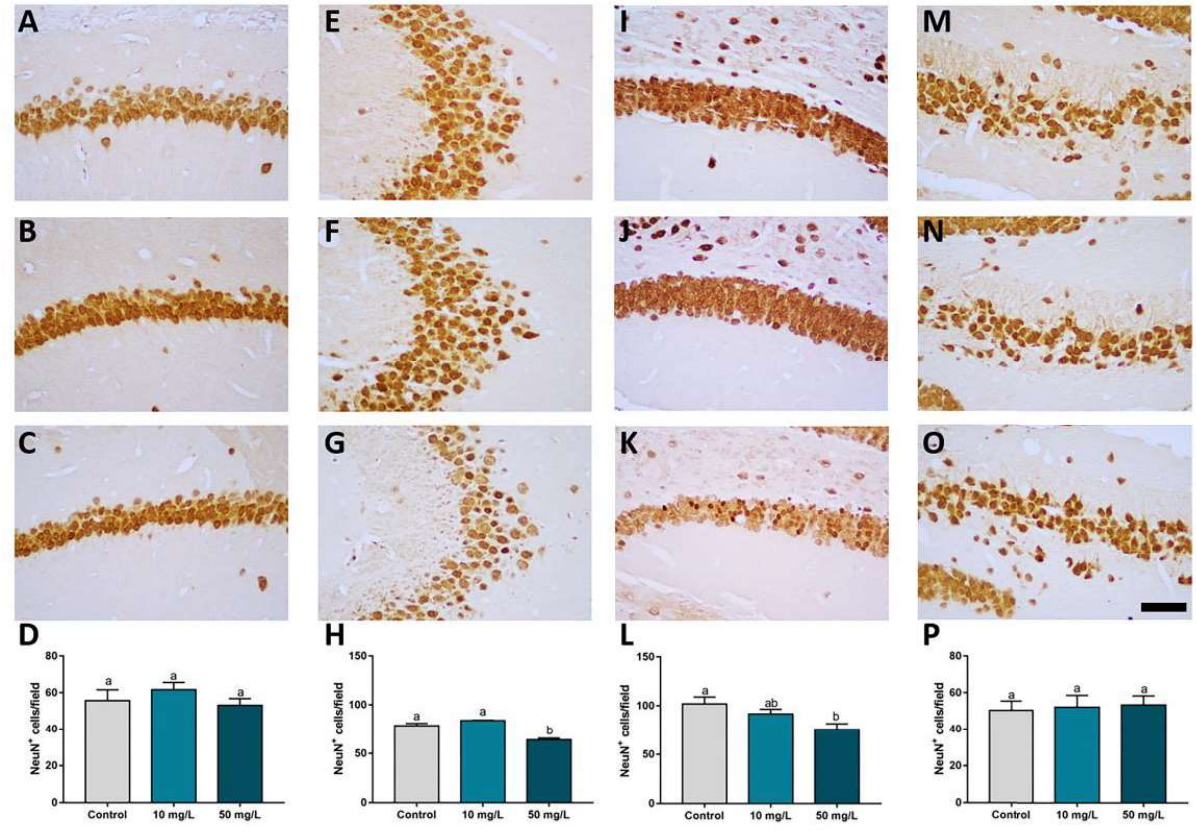

Figure 3. Effects of fluoride exposure from adolescence to adulthood in the mature neurons' density in hippocampus of mice. Immunohistochemistry performed by anti-NeuN labeling in CA1 (A-D), CA3 (E-H), Dentate Gyrus (I-L) and Hilus (M-P) of mice hippocampus. Data are presented as mean ± S.E.M of the neuron density. Different overwritten letters indicate statistical difference (p<0.05, One-way ANOVA with Tukey's post-hoc test). Scale bar: 50µm.

3.4. EXPOSURE TO HIGH F CONCENTRATIONS FOR 60 DAYS IS CAPABLE OF DAMAGING COGNITIVE PARAMETERS IN MICE EXPOSED FROM ADOLESCENCE TO ADULTHOOD

The aversive memory by step-down inhibitory avoidance test showed that both short-term (adj. p value = 0.0005; Fig. 4A) and long-term (adj. p value = 0.03; Fig. 4B) memories were impaired after 50 mg/L of fluoride exposure. No damages were observed in the 10 mg/L group (p>0.05).

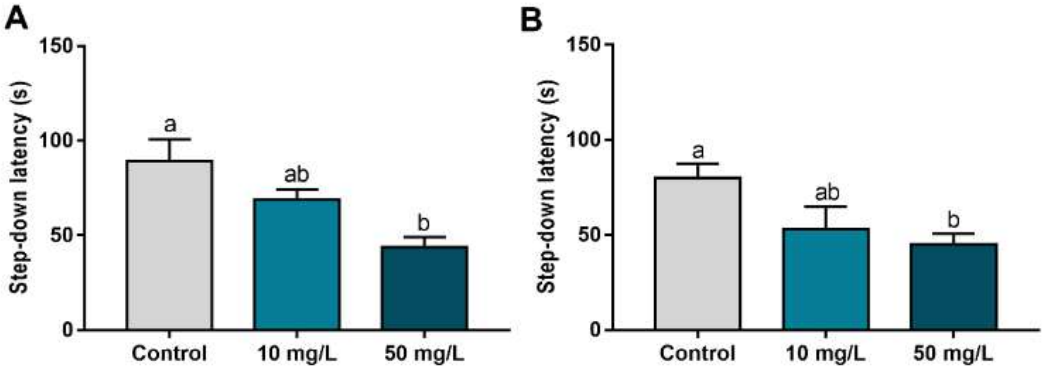

Figure 4. Effects of fluoride exposure from adolescence to adulthood on step-down inhibitory avoidance test performance of mice. In A and B, step-down latency (seconds) in the short-term (1.5h) and long-term (24h) memory assessments, respectively. Different overwritten letters indicate statistical difference (p<0.05, One-way ANOVA with Tukey's post-hoc test).

Regarding the spatial memory, during the training phase, the animals in the 50 mg/L group showed poorer performance compared to the control and 10 mg/L groups (adj. p value < 0.0001), requiring more time to reach the target quadrant after 3 training sessions (Fig. 4B). When assessing a learning parameter (Fig. 4D), long-term exposure to 50 mg/L F reduced the time spent in Q4 in comparison to control (adj. p value = 0.01).

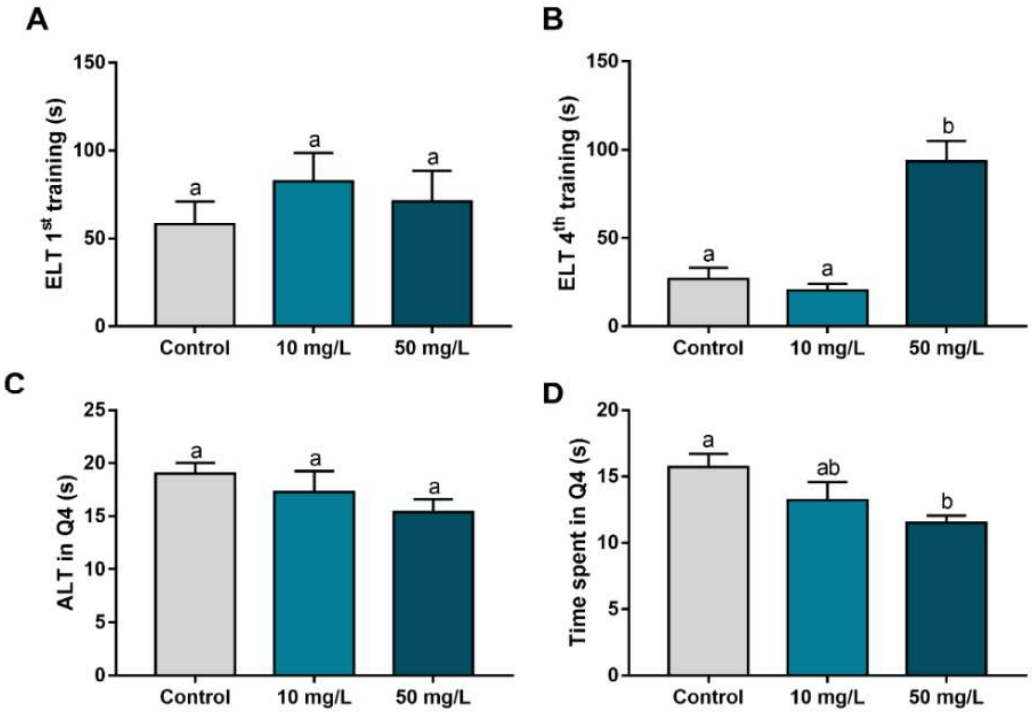

Figure 5. Effects of fluoride exposure from adolescence to adulthood on Water Maze test performance of mice. In A and B, Escape Latency Time (ELT, seconds) in 1st and 4th training sessions, respectively. In C, Arrival Latency Time (ALT, seconds) in the target (Q4) and in D, Time Spent (seconds) in the target (Q4). Different overwritten letters indicate statistical difference ($p<0.05$, One-way ANOVA with Tukey's post-hoc test).

4. DISCUSSION

This study evidenced that the long-term exposure to high concentrations of fluoride can trigger damages to cognitive functions associated with the hippocampus in mice exposed from adolescence to adulthood. The results pointed that, underlying the short- and long-term memories impairment, a neurodegenerative pattern in CA3 and DG regions from hippocampus is triggered, besides an intense global proteomic profile modulation of proteins related to synaptic function, neuroplasticity and energy metabolism. No functional impairments were observed in mice exposed to low concentrations, even with increased fluoride bioavailability and proteome modulation.

We designed our experimental model based on three main points: The animals' age, once we begun to exposed them to fluoride at age of 21 days; The concentrations elected, once it has a translational relevance because the lower one (10 mg/L) is equivalent to the levels found in water supply artificially fluoridated, and the higher (50 mg/L), equivalent to regions with endemic fluorosis [19]; and the long-term exposure model, both adapted to rodent's metabolism [18], that lasts from adolescence to the adult stage of animals. Thus, to validate our exposure model, we assessed the fluoride

plasma levels, which showed an increase on fluoride plasma bioavailability in the exposed animals, being in accordance with previous publications that also evidenced damages to the hippocampus of rats exposed during the intrauterine and lactational periods [15], and in the cerebellum [14] and salivary glands [33] of adult mice.

It is well known that mammals' brains continue to develop even after birth, and for this reason, the CNS is susceptible to xenobiotic damages in this period [34]. At the age of 21 days until 60 days old, mice brain undergoes through several modifications and reach total maturation, and as reviewed by Semple et al. [35], this period corresponds to humans with 2 to 20 years old, due the similarities of developmental events that occurs in both species, as peak in synaptic density, in myelination rate, refinement of cognitive-dependent circuitry, synaptic density adult levels and others [35]. In this way, several observational studies have pointed to the neurodevelopmental toxic effects of fluoride exposure (for review see Choi et al. [36]; and Grandjean [37]). Thus, these points reinforce the representativeness of our study, especially considering the dichotomy between the fluoridation of water supply and the environment toxicological concern, and provides reliable evidences to literature regarding pre-clinical outcomes associated with fluoride long-term exposure.

We evaluated different biological organizational levels, as molecular, morphological and functional aspects from hippocampus, a pivotal structure from central nervous system (CNS) involved in cognitive processes as memory and learning. Cognitive functions are defined as a set of abilities related to emotions, communication, hearing processing, decision making, learning and memories [38] These two last components involve complex molecular processes and anatomical structures, which allow the subdivision according to the duration (short – and long-term) and content (declarative or procedural), for example [39]. In the step-down inhibitory avoidance task, the amygdala is an important anatomical region due the emotional aspect in this test, however the hippocampus is pivotal for memory formation [20], on the other hand, in the water maze test, the spatial memory formation and learning processes are mediated, mainly, by the hippocampus [40]. Thus, we elected the hippocampus as the region of interest due to its importance in both ethological approaches and the results evidenced damages to short- and long-term memories in the step-down inhibitory avoidance trial, and on long-term memory and learning abilities by the Morris' water maze test, triggered by high fluoride concentration exposure.

The neurotoxic effects of fluoride have been attributed to several mechanisms, as metabolic impairment, oxidative stress, neuroinflammation, apoptosis [41]. Previous publications showed a decrease on ATP synthesis and a decrease on reduced glutathione and oxidized glutathione ration in glial-like cells after fluoride exposure [42], increase on oxidative stress markers, as lipid peroxidation and nitrites, in the cerebellum of adult mice and hippocampus of rats exposed to fluoride during the gestational period [14,15]. Besides that, the neuroinflammatory profile triggered by fluoride has been associated with the microglial activation, increase on interleukin-1β, interleukin-6 and tumor necrosis factor-α in hippocampus [43,44]. These molecular and biochemical features may culminate into reduced cell viability and cell death by autophagy and apoptosis [45,46], resulting into a neurodegenerative process and loss of neural function.

In this perspective, we analyzed the neuronal density from four regions from dorsal hippocampus: CA1, CA3, hilus and DG. No morphological changes were observed in CA1 and hilus, but the significative damages observed on CA3 and DG seems to be associated with the cognitive impairments triggered by 50 mg/L of fluoride exposure. The DG acts as an input link between the entorhinal cortex and the hippocampus, and a site of projections from the hippocampus to others brain areas [47], and the CA3, also receives inputs from the entorhinal cortex by the perforant path and from the DG by the mossy fiber [48], which compose the anatomical pathways involved in hippocampal-related memories.

Previous publications investigated the possible damages triggered by fluoride, however, the majority used different ages, and higher fluoride concentrations. Two studies in particular assessed the global proteomic profile of rat exposed to 100 mg/L of fluoride [49] and to 20mg/kg/day of NaF (i.p.) for 30 days [50] which may be interesting to elucidate mechanisms of fluoride neurotoxicity, but face some important limitations regarding the translational point of view in the justificative of dose and temporal exposure window.

Our proteomic approach showed that fluoride exposure modulates the hippocampal proteome at both concentrations, and interestingly, several proteins were commonly found in both comparisons and with different status of regulation. The over-representation analysis allows to investigate the common biological processes among the three comparisons performed in the proteomic approach, and revealed that some of those common proteins are mainly related to cellular component organization,

nervous system development, response to stimulus, metabolic process, nervous system process and synaptic signaling. In this way, we suggest that the different pattern of response after the exposure to low and high fluoride levels may site on those biological processes.

The first set of proteins that must be discussed are involved in the response to stimulus, that play an important role in the different patterns of response between exposed groups. The heat shock proteins (HSP) are molecular chaperones involved in the processes of oxidative stress signaling, transcription processes, protein maturation and re-folding, and degradation [51]. Those proteins were suggested elsewhere [52] as possible new therapeutical tools, being associated with neurodegenerative diseases [53], and part of neurodevelopment by mediating cell growth and migration, axon guidance, and angiogenesis [54]. The exposure to 10 mg/L caused down-regulation of HSP *70 kDa protein 1B* (P17879), *70 kDa protein 1-like* (P16627); up-regulation of *75 kDa, mitochondrial* (Q9CQN1) and *90 kDa-beta* (P11499); exclusive expression of *70 kDa protein 4* (Q61316), *70 kDa protein 4L* (P48722) and *105 kDa* (Q61699) in exposed group. On the other hand, the 50 mg/L caused down-regulation of P16627, *HSP 71 kDa protein* (P63017), *70 kDa protein 2* (P17156); and up-regulation of Q9CQN1 and *HSP 90-alpha* (P07901). This proteomic modulation may be associated with a response to the damages triggered by fluoride exposure and even a compromise on hippocampal neurodevelopment.

As mentioned before, in addition to serving as a marker of proteome protection or damage, HSPs are also important markers in oxidative stress [55]. In this perspective, the proteomic approach also revealed the significant modulation of antioxidant enzymes, such as the up-regulation of *Glutathione S-transferase Mu 1, 2* and *7* (P10649, P15626 and Q80W21, respectively), *Peroxiredoxin-2* (Q61171), *and Superoxide dismutase* [Cu-Zn] (P08228); and the exclusive expression of *Glutathione S-transferase P 1* and *2* (P19157 and P46425, respectively) in 10 mg/L group. Also, it was observed the exclusive regulation of *Peroxiredoxin-1* (P35700), *Peroxiredoxin-4* (O08807) in 10 mg/L group. In the 50 mg/L, the proteins P15626 and Q80W21 were also up-regulated in comparison to control, in addition to *Glutathione S-transferase Mu 5* (P48774) and *Peroxiredoxin-5*, *mitochondrial* (P99029). The proteins P35700 and O08807 were found exclusively expressed in 50 mg/L. These findings suggest a positive response of the enzymatic antioxidant system against reactive oxygen species in the hippocampus of mice exposed to 10 mg/L and 50 mg/L of fluoride. The changes

on these proteins, and others components from antioxidant system, are associated with the fluoride-induced oxidative stress, one of the fluoride mechanisms of damage [44].

In fact, the execution of neural functions is dependent on several structural components, molecular pathways and neurochemical communication. In this perspective, based on the over-representation analysis, we can highlight three biological processes: Cellular component organization, Nervous system process and synaptic signaling, which presented cytoskeletal proteins, synaptosome components, and proteins related to dendritic organization.

The cytoskeleton rearrangement plays a key role in the process of transporting synaptic vesicles [56], besides the maintenance of cell morphology, and both actin filaments and microtubules had their structural components significantly altered. Several *Tubulin alpha* and *beta chains* (see supplementary tables 2 and 3) were found up-regulated in 10 mg/L group, but down-regulated in 50 mg/L group. This may indicate an important impairment on microtubule function, once this cytoskeleton component is important to maintain the cell shape, dendritic morphogenesis and the intracellular tracking of vesicles [57].

Moreover, actin filaments are well known as participants of many biological processes, such as cell migration and division, but are also determinants in the formation of dendritic spikes and consequent long-term memory consolidation, and also participate actively in neuronal exocytosis and endocytosis process [56,58,59]. Interestingly, this cytoskeleton component had an opposite profile in comparison to microtubule constituents. Several actin isoforms were down-regulated in 10 mg/L group, and up-regulated in 50 mg/L, such as *Actin, alpha cardiac muscle 1* (P68033), *Actin, alpha skeletal muscle* (P68134), *Actin, aortic smooth muscle* (P62737) and *Actin, gamma-enteric smooth muscle* (P63268). This up-regulation profile of actin filaments is often found in reactive astrocytes and may indicate astrocyte reactivity to an injury triggered by fluoride.

Other set of proteins directly associated with the cytoskeleton, is the *microtubule associated protein (MAP)* group, which acts as stabilizers of microtubules [60]. The proteomic approach revealed the up-regulation of *MAP 2* (P20357; up-regulated in 10 mg/L group in comparison to control) and *MAP 1A* and *6* (Q9QYR6 and Q7TSJ2, respectively) exclusive expression in 10 mg/L in comparison to control. The Q9QYR6 was found exclusively in 50 mg/L group in comparison to control, but down-regulated

in comparison to 10 mg/L group. Besides, when it comes to neurons, the MAP is important to maintain the synaptic plasticity [61] along with other proteins such as *Postsynaptic density proteins 93* and *95*, also known as *Disk Large Homolog 2* (Q91XM9) and 4 (Q62108), respectively besides the *Synaptophysin* (Q62277), composing the pre- and post-synaptic platforms and synaptic vesicle [62-64]. The 10 mg/L group showed exclusive regulation of Q91XM9 and Q62108 in exposed group, and down-regulation of (Q62277) in comparison to control, and unique in 10mg/L group in comparison to 50 mg/L. This profile suggests that the lower fluoride concentration triggered an increase on synaptic activity, and the higher concentration, a reduced synaptic activity, which may explain the behavioral results found.

Following this perspective, the exposure to 10 mg/L caused down-regulation of Calcium/calmodulin-dependent protein kinase type II subunits alpha (P11798) and beta (P28652), Calmodulin-1, 2 and 3 (P0DP26, P0DP27 and P0DP28, respectively), while the 50 mg/L, caused up-regulation of them. This protein complex plays several biological roles involving the calcium signaling pathways, as synaptic plasticity [65]. It is known as one of the major set of proteins present in post-synaptic platform, and is involved in cognitive functions as memory and learning [66,67].

In this way, underlying the functional impairments observed in the behavioral assessment, and the molecular and morphological features, the long-term exposure to fluoride seems to be associated with an intense modulation of proteins related to synaptic transmission, by increasing the regulation some synaptosome components when mice are exposed to 10 mg/L, and an opposite pattern when exposed to 50 mg/L. Besides this scenario, the neurodegeneration found in hippocampal regions are also indicative of how long-term exposure to high concentrations of fluoride may trigger cognitive damages.

5. CONCLUSIONS

In conclusion, the fluoride long-term exposure to optimal levels by artificially fluoridated water is not associated with cognitive impairments, while the high concentration exposure triggered memory and learning deficits, associated with a neurodegenerative pattern. Our results point to new investigations in longer times and at different ages to better elucidate whether the molecular alterations found at 10 mg/L are really harmless to cognitive function.

DECLARATION OF COMPETING INTEREST

The authors declared no conflict of interest

FINANCIAL STATEMENT

L.O.B thanks to Conselho Nacional de Desenvolvimento Científico e Tecnológico (CNPq) for the graduation scholarship. The APC was founded by Pró-reitoria de Pesquisa e Pós-graduação from Federal University of Pará. C.S.F.M and M.A.R.B. thank CNPq for the research productivity scholarship.

SUPPLEMENTARY DATA

Supplementary table 1. Complete list of biological processes according to Gene Ontology of the proteins found modulated between group comparisons.

Supplementary table 2. Identified proteins with expression significantly altered in the hippocampus of mice control group vs. 10 mg/L group.

Supplementary table 3. Identified proteins with expression significantly altered in the hippocampus of mice control group vs. 50 mg/L group.

Supplementary table 4. Identified proteins with expression significantly altered in the hippocampus of mice 50 mg/L group vs. 10 mg/L group.

CREDIT AUTHOR CONTRIBUTION STATEMENT

Conceptualization: R.R.L., L.O.B.; Formal analysis: L.O.B., B.P., C.S.F.M., R.R.L.; Funding acquisition: R.R.L; Investigation: R.R.L., C.S.F.M, M.A.R.B.; Methodology: L.O.B., M.K.F., W.A.A.B., A.D., L.M.P.F., S.C.C., L.Y.; Project administration: R.R.L.; Supervision: R.R.L., C.S.F.M. Writing– original draft: L.O.B., A.D.; Writing– review & editing: C.S.F.M., L.M.P.F., M.A.R.B, R.R.L.

REFERENCES

1. Ando, M.; Tadano, M.; Yamamoto, S.; Tamura, K.; Asanuma, S.; Watanabe, T.; Kondo, T.; Sakurai, S.; Ji, R.; Liang, C.; et al. Health effects of fluoride pollution caused by coal burning. *The Science of the total environment* **2001**, *271*, 107-116, doi:10.1016/s0048-9697(00)00836-6.
2. Kanduti, D.; Sterbenk, P.; Artnik, B. FLUORIDE: A REVIEW OF USE AND EFFECTS ON HEALTH. *Materia socio-medica* **2016**, *28*, 133-137, doi:10.5455/msm.2016.28.133-137.
3. Tenuta, L.M.; Cury, J.A. Fluoride: its role in dentistry. *Brazilian oral research* **2010**, *24 Suppl 1*, 9-17, doi:10.1590/s1806-83242010000500003.

4. Mullen, J. History of water fluoridation. *British dental journal* **2005**, *199*, 1-4, doi:10.1038/sj.bdj.4812863.
5. Organization, W.H. WHO Guidelines Approved by the Guidelines Review Committee. In *Guidelines for Drinking-Water Quality: Fourth Edition Incorporating the First Addendum*; World Health Organization

6. Fawell, J.; Bailey, K.; Chilton, J.; Dahi, E.; Magara, Y. *Fluoride in drinking-water*; IWA publishing: 2006.
7. Guth, S.; Hüser, S.; Roth, A.; Degen, G.; Diel, P.; Edlund, K.; Eisenbrand, G.; Engel, K.-H.; Epe, B.; Grune, T.; et al. Toxicity of fluoride: critical evaluation of evidence for human developmental neurotoxicity in epidemiological studies, animal experiments and in vitro analyses. *Archives of Toxicology* **2020**, *94*, 1375-1415, doi:10.1007/s00204-020-02725-2.
8. Zuo, H.; Chen, L.; Kong, M.; Qiu, L.; Lü, P.; Wu, P.; Yang, Y.; Chen, K. Toxic effects of fluoride on organisms. *Life sciences* **2018**, *198*, 18-24, doi:10.1016/j.lfs.2018.02.001.
9. Choi, A.L.; Sun, G.; Zhang, Y.; Grandjean, P. Developmental Fluoride Neurotoxicity: A Systematic Review and Meta-Analysis. **2012**, *120*, 1362-1368, doi:doi:10.1289/ehp.1104912.
10. Duan, Q.; Jiao, J.; Chen, X.; Wang, X. Association between water fluoride and the level of children's intelligence: a dose-response meta-analysis. *Public health* **2018**, *154*, 87-97, doi:10.1016/j.puhe.2017.08.013.
11. Miranda, G.H.N.; Alvarenga, M.O.P.; Ferreira, M.K.M.; Puty, B.; Bittencourt, L.O.; Fagundes, N.C.F.; Pessan, J.P.; Buzalaf, M.A.R.; Lima, R.R. A systematic review and meta-analysis of the association between fluoride exposure and neurological disorders. *Scientific Reports* **2021**.
12. Yeung, C.A. A systematic review of the efficacy and safety of fluoridation. *Evidence-based dentistry* **2008**, *9*, 39-43, doi:10.1038/sj.ebd.6400578.
13. Dionizio, A.S.; Melo, C.G.S.; Sabino-Arias, I.T.; Ventura, T.M.S.; Leite, A.L.; Souza, S.R.G.; Santos, E.X.; Heubel, A.D.; Souza, J.G.; Perles, J.V.C.M.; et al. Chronic treatment with fluoride affects the jejunum: insights from proteomics and enteric innervation analysis. *Scientific Reports* **2018**, *8*, 3180, doi:10.1038/s41598-018-21533-4.
14. Lopes, G.O.; Martins Ferreira, M.K.; Davis, L.; Bittencourt, L.O.; Bragança Aragão, W.A.; Dionizio, A.; Rabelo Buzalaf, M.A.; Crespo-Lopez, M.E.; Maia, C.S.F.; Lima, R.R. Effects of Fluoride Long-Term Exposure over the Cerebellum: Global Proteomic Profile, Oxidative Biochemistry, Cell Density, and Motor Behavior Evaluation. *International journal of molecular sciences* **2020**, *21*, doi:10.3390/ijms21197297.
15. Ferreira, M.K.M.; Aragão, W.A.B.; Bittencourt, L.O.; Puty, B.; Dionizio, A.; Souza, M.P.C.; Buzalaf, M.A.R.; de Oliveira, E.H.; Crespo-Lopez, M.E.; Lima, R.R. Fluoride exposure during pregnancy and lactation triggers oxidative stress and molecular changes in hippocampus of offspring rats. *Ecotoxicology and environmental safety* **2021**, *208*, 111437, doi:10.1016/j.ecoenv.2020.111437.
16. Dionizio, A.; Uyghurturk, D.A.; Melo, C.G.S.; Sabino-Arias, I.T.; Araujo, T.T.; Ventura, T.M.S.; Perles, J.; Zanoni, J.N.; Den Besten, P.; Buzalaf, M.A.R. Intestinal changes associated with fluoride exposure in rats: Integrative morphological, proteomic and microbiome analyses. *Chemosphere* **2021**, *273*, 129607, doi:10.1016/j.chemosphere.2021.129607.

17. Pereira, H.; Araújo, T.T.; Dionizio, A.; Trevizol, J.S.; Pereira, F.S.; Iano, F.G.; Faria Ximenes, V.; Buzalaf, M.A.R. Increase of complex I and reduction of complex II mitochondrial activity are possible adaptive effects provoked by fluoride exposure. *Heliyon* **2021**, *7*, e06028, doi:10.1016/j.heliyon.2021.e06028.
18. Dunipace, A.J.; Brizendine, E.J.; Zhang, W.; Wilson, M.E.; Miller, L.L.; Katz, B.P.; Warrick, J.M.; Stookey, G.K. Effect of aging on animal response to chronic fluoride exposure. *Journal of dental research* **1995**, *74*, 358-368, doi:10.1177/00220345950740011201.
19. Miranda, G.H.N.; Gomes, B.A.Q.; Bittencourt, L.O.; Aragão, W.A.B.; Nogueira, L.S.; Dionizio, A.S.; Buzalaf, M.A.R.; Monteiro, M.C.; Lima, R.R. Chronic Exposure to Sodium Fluoride Triggers Oxidative Biochemistry Misbalance in Mice: Effects on Peripheral Blood Circulation. *Oxidative medicine and cellular longevity* **2018**, *2018*, 8379123, doi:10.1155/2018/8379123.
20. Izquierdo, I.; Medina, J.H. Memory formation: the sequence of biochemical events in the hippocampus and its connection to activity in other brain structures. *Neurobiology of learning and memory* **1997**, *68*, 285-316, doi:10.1006/nlme.1997.3799.
21. Alves Oliveira, A.C.; Dionizio, A.; Teixeira, F.B.; Bittencourt, L.O.; Nonato Miranda, G.H.; Oliveira Lopes, G.; Varela, E.L.P.; Nabiça, M.; Ribera, P.; Dantas, K.; et al. Hippocampal Impairment Triggered by Long-Term Lead Exposure from Adolescence to Adulthood in Rats: Insights from Molecular to Functional Levels. *International journal of molecular sciences* **2020**, *21*, doi:10.3390/ijms21186937.
22. Silva, M.L.; Luz, D.A.; Paixão, T.P.; Silva, J.P.; Belém-Filho, I.J.; Fernandes, L.M.; Gonçalves, A.C.; Fontes-Júnior, E.A.; de Andrade, M.A.; Maia, C.S. Petiveria alliacea exerts mnemonic and learning effects on rats. *Journal of ethnopharmacology* **2015**, *169*, 124-129, doi:10.1016/j.jep.2015.04.005.
23. Bittencourt, L.O.; Dionizio, A.; Nascimento, P.C.; Puty, B.; Leão, L.K.R.; Luz, D.A.; Silva, M.C.F.; Amado, L.L.; Leite, A.; Buzalaf, M.R.; et al. Proteomic approach underlying the hippocampal neurodegeneration caused by low doses of methylmercury after long-term exposure in adult rats. *Metallomics : integrated biometal science* **2019**, *11*, 390-403, doi:10.1039/c8mt00297e.
24. Taves, D.R. Separation of fluoride by rapid diffusion using hexamethyldisiloxane. *Talanta* **1968**, *15*, 969-974, doi:10.1016/0039-9140(68)80097-9.
25. Whitford, G.M. *The metabolism and toxicity of fluoride*; Karger Publishers: 1996.
26. Bittencourt, L.O.; Puty, B.; Charone, S.; Aragão, W.A.B.; Farias-Junior, P.M.; Silva, M.C.F.; Crespo-Lopez, M.E.; Leite, A.L.; Buzalaf, M.A.R.; Lima, R.R. Oxidative Biochemistry Disbalance and Changes on Proteomic Profile in Salivary Glands of Rats Induced by Chronic Exposure to Methylmercury. *Oxidative medicine and cellular longevity* **2017**, *2017*, 5653291, doi:10.1155/2017/5653291.
27. Bradford, M.M. A rapid and sensitive method for the quantitation of microgram quantities of protein utilizing the principle of protein-dye binding. *Analytical biochemistry* **1976**, *72*, 248-254, doi:10.1006/abio.1976.9999.
28. Bindea, G.; Mlecnik, B.; Hackl, H.; Charoentong, P.; Tosolini, M.; Kirilovsky, A.; Fridman, W.H.; Pagès, F.; Trajanoski, Z.; Galon, J. ClueGO: a Cytoscape plug-in to decipher functionally grouped gene ontology and pathway

annotation networks. *Bioinformatics (Oxford, England)* **2009**, *25*, 1091-1093, doi:10.1093/bioinformatics/btp101.
29. Eiró, L.G.; Ferreira, M.K.M.; Bittencourt, L.O.; Aragão, W.A.B.; Souza, M.P.C.; Silva, M.C.F.; Dionizio, A.; Buzalaf, M.A.R.; Crespo-López, M.E.; Lima, R.R. Chronic methylmercury exposure causes spinal cord impairment: Proteomic modulation and oxidative stress. *Food and chemical toxicology : an international journal published for the British Industrial Biological Research Association* **2020**, *146*, 111772, doi:10.1016/j.fct.2020.111772.
30. Alhamdoosh, M.; Ng, M.; Wilson, N.J.; Sheridan, J.M.; Huynh, H.; Wilson, M.J.; Ritchie, M.E.J.B. Combining multiple tools outperforms individual methods in gene set enrichment analyses. **2017**, *33*, 414-424.
31. Shannon, P.; Markiel, A.; Ozier, O.; Baliga, N.S.; Wang, J.T.; Ramage, D.; Amin, N.; Schwikowski, B.; Ideker, T. Cytoscape: a software environment for integrated models of biomolecular interaction networks. *Genome research* **2003**, *13*, 2498-2504, doi:10.1101/gr.1239303.
32. Xia, J.; Benner, M.J.; Hancock, R.E. NetworkAnalyst--integrative approaches for protein-protein interaction network analysis and visual exploration. *Nucleic acids research* **2014**, *42*, W167-174, doi:10.1093/nar/gku443.
33. Lima, L.A.O.; Miranda, G.H.N.; Aragão, W.A.B.; Bittencourt, L.O.; Dos Santos, S.M.; de Souza, M.P.C.; Nogueira, L.S.; de Oliveira, E.H.C.; Monteiro, M.C.; Dionizio, A.; et al. Effects of Fluoride on Submandibular Glands of Mice: Changes in Oxidative Biochemistry, Proteomic Profile, and Genotoxicity. *Frontiers in pharmacology* **2021**, *12*, 715394, doi:10.3389/fphar.2021.715394.
34. Rock, K.D.; Patisaul, H.B. Environmental Mechanisms of Neurodevelopmental Toxicity. *Current environmental health reports* **2018**, *5*, 145-157, doi:10.1007/s40572-018-0185-0.
35. Semple, B.D.; Blomgren, K.; Gimlin, K.; Ferriero, D.M.; Noble-Haeusslein, L.J. Brain development in rodents and humans: Identifying benchmarks of maturation and vulnerability to injury across species. *Progress in neurobiology* **2013**, *106-107*, 1-16, doi:10.1016/j.pneurobio.2013.04.001.
36. Choi, A.L.; Sun, G.; Zhang, Y.; Grandjean, P. Developmental fluoride neurotoxicity: a systematic review and meta-analysis. *Environmental health perspectives* **2012**, *120*, 1362-1368, doi:10.1289/ehp.1104912.
37. Grandjean, P. Developmental fluoride neurotoxicity: an updated review. *Environmental health : a global access science source* **2019**, *18*, 110, doi:10.1186/s12940-019-0551-x.
38. Fernandes, R.M.; Correa, M.G.; Dos Santos, M.A.R.; Almeida, A.; Fagundes, N.C.F.; Maia, L.C.; Lima, R.R. The Effects of Moderate Physical Exercise on Adult Cognition: A Systematic Review. *Frontiers in physiology* **2018**, *9*, 667, doi:10.3389/fphys.2018.00667.
39. Vianna, M.R.; Izquierdo, L.A.; Barros, D.M.; Walz, R.; Medina, J.H.; Izquierdo, I. Short- and long-term memory: differential involvement of neurotransmitter systems and signal transduction cascades. *Anais da Academia Brasileira de Ciencias* **2000**, *72*, 353-364, doi:10.1590/s0001-37652000000300009.
40. Bird, C.M.; Burgess, N. The hippocampus and memory: insights from spatial processing. *Nature reviews. Neuroscience* **2008**, *9*, 182-194, doi:10.1038/nrn2335.
41. Strunecka, A.; Strunecky, O. Mechanisms of Fluoride Toxicity: From Enzymes to Underlying Integrative Networks. **2020**, *10*, 7100.

42. Puty, B.; Bittencourt, L.O.; Nogueira, I.C.; Buzalaf, M.A.R.; Oliveira, E.H.; Lima, R.R. Human cultured IMR-32 neuronal-like and U87 glial-like cells have different patterns of toxicity under fluoride exposure. *PloS one* **2021**, *16*, e0251200, doi:10.1371/journal.pone.0251200.
43. Yang, L.; Jin, P.; Wang, X.; Zhou, Q.; Lin, X.; Xi, S. Fluoride activates microglia, secretes inflammatory factors and influences synaptic neuron plasticity in the hippocampus of rats. *NeuroToxicology* **2018**, *69*, 108-120, doi:https://doi.org/10.1016/j.neuro.2018.09.006.
44. Shuhua, X.; Ziyou, L.; Ling, Y.; Fei, W.; Sun, G. A role of fluoride on free radical generation and oxidative stress in BV-2 microglia cells. *Mediators of inflammation* **2012**, *2012*, 102954, doi:10.1155/2012/102954.
45. Tu, W.; Zhang, Q.; Liu, Y.; Han, L.; Wang, Q.; Chen, P.; Zhang, S.; Wang, A.; Zhou, X. Fluoride induces apoptosis via inhibiting SIRT1 activity to activate mitochondrial p53 pathway in human neuroblastoma SH-SY5Y cells. *Toxicology and applied pharmacology* **2018**, *347*, 60-69, doi:10.1016/j.taap.2018.03.030.
46. Zhou, G.; Tang, S.; Yang, L.; Niu, Q.; Chen, J.; Xia, T.; Wang, S.; Wang, M.; Zhao, Q.; Liu, L.; et al. Effects of long-term fluoride exposure on cognitive ability and the underlying mechanisms: Role of autophagy and its association with apoptosis. *Toxicology and applied pharmacology* **2019**, *378*, 114608, doi:10.1016/j.taap.2019.114608.
47. Izquierdo, I.; Medina, J.H.; Vianna, M.R.; Izquierdo, L.A.; Barros, D.M. Separate mechanisms for short- and long-term memory. *Behavioural brain research* **1999**, *103*, 1-11, doi:10.1016/s0166-4328(99)00036-4.
48. Cherubini, E.; Miles, R. The CA3 region of the hippocampus: how is it? What is it for? How does it do it? *Frontiers in cellular neuroscience* **2015**, *9*, 19, doi:10.3389/fncel.2015.00019.
49. Ran, L.Y.; Xiang, J.; Zeng, X.X.; Tang, J.L.; Dong, Y.T.; Zhang, F.; Yu, W.F.; Qi, X.L.; Xiao, Y.; Zou, J.; et al. Integrated transcriptomic and proteomic analysis indicated that neurotoxicity of rats with chronic fluorosis may be in mechanism involved in the changed cholinergic pathway and oxidative stress. *Journal of trace elements in medicine and biology : organ of the Society for Minerals and Trace Elements (GMS)* **2021**, *64*, 126688, doi:10.1016/j.jtemb.2020.126688.
50. Pan, Y.; Lü, P.; Yin, L.; Chen, K.; He, Y. Effect of fluoride on the proteomic profile of the hippocampus in rats. *Zeitschrift fur Naturforschung. C, Journal of biosciences* **2015**, *70*, 151-157, doi:10.1515/znc-2014-4158.
51. Ikwegbue, P.C.; Masamba, P.; Oyinloye, B.E.; Kappo, A.P. Roles of Heat Shock Proteins in Apoptosis, Oxidative Stress, Human Inflammatory Diseases, and Cancer. *Pharmaceuticals (Basel, Switzerland)* **2017**, *11*, doi:10.3390/ph11010002.
52. Almeida, M.B.; do Nascimento, J.L.; Herculano, A.M.; Crespo-López, M.E. Molecular chaperones: toward new therapeutic tools. *Biomedicine & pharmacotherapy = Biomedecine & pharmacotherapie* **2011**, *65*, 239-243, doi:10.1016/j.biopha.2011.04.025.
53. Leak, R.K. Heat shock proteins in neurodegenerative disorders and aging. *Journal of cell communication and signaling* **2014**, *8*, 293-310, doi:10.1007/s12079-014-0243-9.

54. Miller, D.J.; Fort, P.E. Heat Shock Proteins Regulatory Role in Neurodevelopment. *Frontiers in neuroscience* **2018**, *12*, 821, doi:10.3389/fnins.2018.00821.
55. Ikwegbue, P.C.; Masamba, P.; Oyinloye, B.E.; Kappo, A.P. Roles of Heat Shock Proteins in Apoptosis, Oxidative Stress, Human Inflammatory Diseases, and Cancer. **2018**, *11*, 2.
56. Gordon-Weeks, P.R.; Fournier, A.E. Neuronal cytoskeleton in synaptic plasticity and regeneration. *Journal of neurochemistry* **2014**, *129*, 206-212, doi:10.1111/jnc.12502.
57. Lasser, M.; Tiber, J.; Lowery, L.A. The Role of the Microtubule Cytoskeleton in Neurodevelopmental Disorders. *Frontiers in cellular neuroscience* **2018**, *12*, 165, doi:10.3389/fncel.2018.00165.
58. Basu, S.; Lamprecht, R. The Role of Actin Cytoskeleton in Dendritic Spines in the Maintenance of Long-Term Memory. *Frontiers in molecular neuroscience* **2018**, *11*, 143, doi:10.3389/fnmol.2018.00143.
59. Kim, C.H.; Lisman, J.E. A role of actin filament in synaptic transmission and long-term potentiation. *The Journal of neuroscience : the official journal of the Society for Neuroscience* **1999**, *19*, 4314-4324, doi:10.1523/jneurosci.19-11-04314.1999.
60. Bodakuntla, S.; Jijumon, A.S.; Villablanca, C.; Gonzalez-Billault, C.; Janke, C. Microtubule-Associated Proteins: Structuring the Cytoskeleton. *Trends in cell biology* **2019**, *29*, 804-819, doi:10.1016/j.tcb.2019.07.004.
61. Takei, Y.; Kikkawa, Y.S.; Atapour, N.; Hensch, T.K.; Hirokawa, N. Defects in Synaptic Plasticity, Reduced NMDA-Receptor Transport, and Instability of Postsynaptic Density Proteins in Mice Lacking Microtubule-Associated Protein 1A. *The Journal of neuroscience : the official journal of the Society for Neuroscience* **2015**, *35*, 15539-15554, doi:10.1523/jneurosci.2671-15.2015.
62. Kwon, S.E.; Chapman, E.R. Synaptophysin regulates the kinetics of synaptic vesicle endocytosis in central neurons. *Neuron* **2011**, *70*, 847-854, doi:10.1016/j.neuron.2011.04.001.
63. Béïque, J.C.; Andrade, R. PSD-95 regulates synaptic transmission and plasticity in rat cerebral cortex. *The Journal of physiology* **2003**, *546*, 859-867, doi:10.1113/jphysiol.2002.031369.
64. Sun, Q.; Turrigiano, G.G. PSD-95 and PSD-93 play critical but distinct roles in synaptic scaling up and down. *The Journal of neuroscience : the official journal of the Society for Neuroscience* **2011**, *31*, 6800-6808, doi:10.1523/jneurosci.5616-10.2011.
65. Pang, Z.P.; Cao, P.; Xu, W.; Südhof, T.C. Calmodulin controls synaptic strength via presynaptic activation of calmodulin kinase II. *The Journal of neuroscience : the official journal of the Society for Neuroscience* **2010**, *30*, 4132-4142, doi:10.1523/jneurosci.3129-09.2010.
66. Ataei, N.; Sabzghabaee, A.M.; Movahedian, A. Calcium/Calmodulin-dependent Protein Kinase II is a Ubiquitous Molecule in Human Long-term Memory Synaptic Plasticity: A Systematic Review. *International journal of preventive medicine* **2015**, *6*, 88, doi:10.4103/2008-7802.164831.
67. Zalcman, G.; Federman, N.; Romano, A. CaMKII Isoforms in Learning and Memory: Localization and Function. *Frontiers in molecular neuroscience* **2018**, *11*, 445, doi:10.3389/fnmol.2018.00445.

SUPPLEMENTARY DATA

Article: Long-term exposure to high concentrations of fluoride during adolescence to adulthood modulates hippocampal proteome and causes cognitive impairments associated with a neurodegenerative pattern in mice

Authors: Leonardo Oliveira Bittencourt, Aline Dionizio, Maria Karolina Martins Ferreira, Walessa Alana Bragança Aragão, Letícia Yoshitome, Sabrina de Carvalho Cartágenes, Luanna Melo Pereira Fernandes, Bruna Puty, Marília Afonso Rabelo Buzalaf, Cristiane do Socorro Ferraz Maia, Rafael Rodrigues Lima*.

***Corresponding author:**

Rafael Rodrigues Lima, PhD

Laboratory of Functional and Structural Biology, Nº 125, Institute of Biological Sciences, Federal University of Pará; Augusto Corrêa street n. 01, Guamá, Belém-Pará 66075-110, Brazil

E-mail: rafalima@ufpa.br

Supplementary table 1. Complete list of biological processes according to Gene Ontology of the proteins found modulated between group comparisons.

Group Comparison	Biological Process	Number of genes (%)
10mg/L vs. Control	Axon guidance	13.92
	Regulation of axonogenesis	12.66
	Dendritic spine morphogenesis	8.86
	Mitochondrial ATP synthesis coupled proton transport	7.59
	Glycolytic process through fructose-6-phosphate	6.33
	Barbed-end actin filament capping	6.33
	Hypothalamus gonadotrophin-releasing hormone neuron development	5.06
	Central nervous system neuron axonogenesis	3.80
	Pyruvate dehydrogenase (NAD+) activity	3.80
	Positive regulation of ryanodine-sensitive calcium-release channel activity	3.80
	Pyruvate kinase activity	2.53
	Positive regulation of dendrite development	2.53
	Axon target recognition	2.53
	Motor neuron axon guidance	2.53
	Positive regulation of natural killer cell differentiation	2.53
	Positive regulation of histone acetylation	2.53
	Negative regulation of histone acetylation	2.53
	Positive regulation of JUN kinase activity	2.53
	Negative regulation of JUN kinase activity	2.53
	Activation of cysteine-type endopeptidase activity involved in apoptotic process by cytochrome c	2.53
	Positive regulation of P-type sodium:potassium-exchanging transporter activity	2.53
50 mg/L vs. Control	Axon guidance	13.5
	Regulation of axonogenesis	10.6
	Mitochondrial ATP synthesis coupled proton transport	6.7
	Regulation of dendritic spine development	6.7
	Transcription corepressor activity	5.8
	Arp2/3 complex-mediated actin nucleation	4.8

	Glycolytic process through fructose-6-phosphate	4.8
	Ryanodine-sensitive calcium-release channel activity	4.8
	Hypothalamus gonadotrophin-releasing hormone neuron development	3.8
	Negative regulation of mRNA splicing, via spliceosome	2.9
	Negative regulation of axonogenesis	2.9
	Motor neuron axon guidance	2.9
	Central nervous system neuron axonogenesis	2.9
	Regulation of alternative mRNA splicing, via spliceosome	1.9
	Retinal cone cell development	1.9
	Collateral sprouting	1.9
	Positive regulation of transcription initiation from RNA polymerase II promoter	1.9
	Positive regulation of dendrite development	1.9
	Nuclear receptor coactivator activity	1.9
	Regulation of axon diameter	1.9
	Regulation of isotype switching	1.9
	cAMP-dependent protein kinase inhibitor activity	1.9
	Regulation of barbed-end actin filament capping	1.9
	High-affinity glutamate transmembrane transporter activity	1.9
	Positive regulation of P-type sodium:potassium-exchanging transporter activity	1.9
	Negative regulation of histone acetylation	1.9
	Calcium-dependent activation of synaptic vesicle fusion	1.9
50 mg/L vs. 10 mg/L	Regulation of axonogenesis	12.6
	Axon guidance	9.5
	Positive regulation of dendritic spine development	9.5
	Arp2/3 complex-mediated actin nucleation	7.4
	Mitochondrial ATP synthesis coupled proton transport	6.3
	Glycolytic process through fructose-6-phosphate	5.3
	Negative regulation of mRNA splicing, via spliceosome	4.2
	Hypothalamus gonadotrophin-releasing hormone neuron development	4.2
	Acetyl-CoA biosynthetic process from pyruvate	4.2
	Pyruvate dehydrogenase (NAD+) activity	4.2
	Retinal cone cell development	3.2
	Regulation of alternative mRNA splicing, via spliceosome	2.1

Negative regulation of dendrite morphogenesis	2.1
Pyruvate kinase activity	2.1
Positive regulation of ATP biosynthetic process	2.1
Regulation of axon diameter	2.1
Histone H3-K14 acetylation	2.1
cAMP-dependent protein kinase inhibitor activity	2.1
Central nervous system projection neuron axonogenesis	2.1
Regulation of isotype switching	2.1
High-affinity glutamate transmembrane transporter activity	2.1
Positive regulation of P-type sodium:potassium-exchanging transporter activity	2.1
Calcium-dependent activation of synaptic vesicle fusion	2.1
Positive regulation of barbed-end actin filament capping	2.1
Auditory receptor cell morphogenesis	2.1

Supplementary table 2. Identified proteins with expression significantly altered in the hippocampus of mice in 10 mg/L vs. control group.

Accession Id[a]	Description	PLGS Score	Fold Change
Q64467	Glyceraldehyde-3-phosphate dehydrogenase, testis-specific	103.28	6.753
Q9CQN1	Heat shock protein 75 kDa, mitochondrial	242.62	3.353
Q8BZQ7	Anaphase-promoting complex subunit 2	49.72	2.974
P15626	Glutathione S-transferase Mu 2	97.07	2.718
Q80W21	Glutathione S-transferase Mu 7	97.07	2.718
Q9DB05	Alpha-soluble NSF attachment protein	54.03	2.586
P29387	Guanine nucleotide-binding protein subunit beta-4	984.78	2.411
P62806	Histone H4	1669.76	2.411
Q61011	Guanine nucleotide-binding protein G(I)/G(S)/G(T) subunit beta-3	150.23	2.363
Q8CGP0	Histone H2B type 3-B	852.51	2.270
Q8CGP2	Histone H2B type 1-P	1013.8	2.248
Q64524	Histone H2B type 2-E	852.51	2.248
Q6ZWY9	Histone H2B type 1-C/E/G	1013.8	2.226
Q8CGP1	Histone H2B type 1-K	1013.8	2.226

P10854	Histone H2B type 1-M	1013.8	2.226
Q9D2U9	Histone H2B type 3-A	852.51	2.226
Q64475	Histone H2B type 1-B	1013.8	2.203
P10853	Histone H2B type 1-F/J/L	1013.8	2.203
Q64478	Histone H2B type 1-H	1013.8	2.203
Q64525	Histone H2B type 2-B	1013.8	2.203
Q6ZPV2	Chromatin-remodeling ATPase INO80	39.29	2.034
P70296	Phosphatidylethanolamine-binding protein 1	944.72	1.974
Q91ZZ3	Beta-synuclein	76.97	1.954
P28663	Beta-soluble NSF attachment protein	133.71	1.916
Q3V132	ADP/ATP translocase 4	49.88	1.859
Q9JJZ2	Tubulin alpha-8 chain	4374.56	1.840
O55042	Alpha-synuclein	477.8	1.786
O08749	Dihydrolipoyl dehydrogenase, mitochondrial	94.03	1.786
P14094	Sodium/potassium-transporting ATPase subunit beta-1	604.37	1.786
Q3UX10	Tubulin alpha chain-like 3	517.77	1.751
P48962	ADP/ATP translocase 1	173.37	1.716
C0HKE5	Histone H2A type 1-G	1343.38	1.682
C0HKE8	Histone H2A type 1-O	1343.38	1.682
Q6GSS7	Histone H2A type 2-A	1343.38	1.682
C0HKE3	Histone H2A type 1-D	1343.38	1.665
C0HKE4	Histone H2A type 1-E	1343.38	1.665
C0HKE9	Histone H2A type 1-P	1343.38	1.665
C0HKE1	Histone H2A type 1-B	1343.38	1.649
Q8CGP5	Histone H2A type 1-F	1343.38	1.649
C0HKE6	Histone H2A type 1-I	1343.38	1.649
C0HKE7	Histone H2A type 1-N	1343.38	1.649
Q64523	Histone H2A type 2-C	1343.38	1.649
Q8BFU2	Histone H2A type 3	1343.38	1.649
O70456	14-3-3 protein sigma	3068.34	1.632
Q8CGP6	Histone H2A type 1-H	1343.38	1.632
Q8R1M2	Histone H2A.J	1343.38	1.632
C0HKE2	Histone H2A type 1-C	1343.38	1.616

Q8CGP7	Histone H2A type 1-K	1343.38	1.600
P39053	Dynamin-1	4943.16	1.584
Q8BZ98	Dynamin-3	81.67	1.568
P13595	Neural cell adhesion molecule 1	40.83	1.553
P46096	Synaptotagmin-1	213.16	1.553
Q9CZU6	Citrate synthase, mitochondrial	136.89	1.537
P16125	L-lactate dehydrogenase B chain	607.14	1.537
P62880	Guanine nucleotide-binding protein G(I)/G(S)/G(T) subunit beta-2	1227.2	1.522
P63328	Serine/threonine-protein phosphatase 2B catalytic subunit alpha isoform	209.5	1.507
Q9WUA3	ATP-dependent 6-phosphofructokinase, platelet type	102.29	1.492
P26443	Glutamate dehydrogenase 1, mitochondrial	717.95	1.492
P61982	14-3-3 protein gamma	3176.03	1.477
P47857	ATP-dependent 6-phosphofructokinase, muscle type	66.63	1.477
P20029	Endoplasmic reticulum chaperone BiP	441.99	1.477
Q9D051	Pyruvate dehydrogenase E1 component subunit beta, mitochondrial	63.62	1.477
O55131	Septin-7	270.57	1.477
P06745	Glucose-6-phosphate isomerase	613.13	1.462
P05201	Aspartate aminotransferase, cytoplasmic	401.64	1.448
Q9Z0E0	Neurochondrin	107.25	1.433
P48453	Serine/threonine-protein phosphatase 2B catalytic subunit beta isoform	91.18	1.433
P39054	Dynamin-2	80.91	1.419
Q9R0P9	Ubiquitin carboxyl-terminal hydrolase isozyme L1	472.01	1.419
P62874	Guanine nucleotide-binding protein G(I)/G(S)/G(T) subunit beta-1	996.97	1.405
P10649	Glutathione S-transferase Mu 1	218.9	1.391
P17427	AP-2 complex subunit alpha-2	212.44	1.363
P62631	Elongation factor 1-alpha 2	167.42	1.363
P43006	Excitatory amino acid transporter 2	262.57	1.363
P50396	Rab GDP dissociation inhibitor alpha	386.95	1.363
Q60932	Voltage-dependent anion-selective channel protein 1	1508.65	1.363
P20357	Microtubule-associated protein 2	267.4	1.350
P09411	Phosphoglycerate kinase 1	194.88	1.350
Q9DD03	Ras-related protein Rab-13	637.26	1.350
P08228	Superoxide dismutase [Cu-Zn]	521.38	1.350

P00342	L-lactate dehydrogenase C chain	515.53	1.336
P62259	14-3-3 protein epsilon	2983.16	1.323
Q6PIE5	Sodium/potassium-transporting ATPase subunit alpha-2	1008.51	1.323
P00405	Cytochrome c oxidase subunit 2	331.92	1.310
Q61598	Rab GDP dissociation inhibitor beta	449.42	1.310
Q60930	Voltage-dependent anion-selective channel protein 2	862.66	1.310
Q6PIC6	Sodium/potassium-transporting ATPase subunit alpha-3	1247.9	1.297
Q9DB20	ATP synthase subunit O, mitochondrial	1284.26	1.284
P11499	Heat shock protein HSP 90-beta	347.11	1.284
P06151	L-lactate dehydrogenase A chain	718.83	1.284
Q9CZT8	Ras-related protein Rab-3B	641.75	1.284
Q9D0M3	Cytochrome c1, heme protein, mitochondrial	154.1	1.271
Q01768	Nucleoside diphosphate kinase B	330.98	1.271
Q8VEM8	Phosphate carrier protein, mitochondrial	303.54	1.271
P62821	Ras-related protein Rab-1A	1356.49	1.271
P35276	Ras-related protein Rab-3D	697.93	1.271
P46460	Vesicle-fusing ATPase	225.46	1.271
Q9CZ13	Cytochrome b-c1 complex subunit 1, mitochondrial	232.11	1.259
P63011	Ras-related protein Rab-3A	1170.72	1.259
P62823	Ras-related protein Rab-3C	641.75	1.259
P55258	Ras-related protein Rab-8A	1356.49	1.259
Q9CQV8	14-3-3 protein beta/alpha	3251.5	1.246
P30275	Creatine kinase U-type, mitochondrial	521.45	1.246
P12787	Cytochrome c oxidase subunit 5A, mitochondrial	1359.6	1.246
P61027	Ras-related protein Rab-10	1356.49	1.246
Q8K386	Ras-related protein Rab-15	1273.06	1.246
P61028	Ras-related protein Rab-8B	1356.49	1.246
P62814	V-type proton ATPase subunit B, brain isoform	95.93	1.246
Q9D1G1	Ras-related protein Rab-1B	1356.49	1.234
Q504M8	Ras-related protein Rab-26	1356.49	1.234
Q6PHN9	Ras-related protein Rab-35	1356.49	1.234
Q8CG50	Ras-related protein Rab-43	1356.49	1.234
O35963	Ras-related protein Rab-33B	1196.69	1.221

P63101	14-3-3 protein zeta/delta	4286.07	1.209
Q923T9	Calcium/calmodulin-dependent protein kinase type II subunit gamma	1360.71	1.209
Q61171	Peroxiredoxin-2	770.66	1.209
Q923S9	Ras-related protein Rab-30	1356.49	1.209
Q8BHD0	Ras-related protein Rab-39A	1310.98	1.209
P01831	Thy-1 membrane glycoprotein	202.4	1.209
P02089	Hemoglobin subunit beta-2	1971.96	1.197
P16546	Spectrin alpha chain, non-erythrocytic 1	133.67	1.197
P63038	60 kDa heat shock protein, mitochondrial	125.91	1.174
P19783	Cytochrome c oxidase subunit 4 isoform 1, mitochondrial	321.26	1.174
P15532	Nucleoside diphosphate kinase A	330.98	1.174
Q62261	Spectrin beta chain, non-erythrocytic 1	118.82	1.150
P97427	Dihydropyrimidinase-related protein 1	1567.8	1.094
Q61595	Kinectin	239.12	-0.167
O70167	Phosphatidylinositol 4-phosphate 3-kinase C2 domain-containing subunit gamma	116.13	-0.228
P02088	Hemoglobin subunit beta-1	3543.4	-0.323
P01942	Hemoglobin subunit alpha	2208.07	-0.343
P02104	Hemoglobin subunit epsilon-Y2	1971.96	-0.353
P61164	Alpha-centractin	251.17	-0.387
P68372	Tubulin beta-4B chain	28843.51	-0.387
P99024	Tubulin beta-5 chain	35888.25	-0.399
P68134	Actin, alpha skeletal muscle	24717.44	-0.403
P60202	Myelin proteolipid protein	5128.56	-0.403
Q9ERD7	Tubulin beta-3 chain	25756.16	-0.407
P68373	Tubulin alpha-1C chain	11309.22	-0.411
Q7TMM9	Tubulin beta-2A chain	37520.65	-0.411
P62737	Actin, aortic smooth muscle	24551.85	-0.415
P68369	Tubulin alpha-1A chain	12359.69	-0.415
P05064	Fructose-bisphosphate aldolase A	3093.45	-0.419
Q8R5C5	Beta-centractin	251.17	-0.423
P05214	Tubulin alpha-3 chain	7666.05	-0.423
O08553	Dihydropyrimidinase-related protein 2	6913.4	-0.427
Q9DC51	Guanine nucleotide-binding protein G(i) subunit alpha	1623.52	-0.427

B2RSH2	Guanine nucleotide-binding protein G(i) subunit alpha-1	1623.52	-0.432
P08752	Guanine nucleotide-binding protein G(i) subunit alpha-2	1623.52	-0.432
Q8CGK7	Guanine nucleotide-binding protein G(olf) subunit alpha	1628.32	-0.432
P17156	Heat shock-related 70 kDa protein 2	933.05	-0.463
P16330	2',3'-cyclic-nucleotide 3'-phosphodiesterase	887.7	-0.482
P11798	Calcium/calmodulin-dependent protein kinase type II subunit alpha	4430.82	-0.487
P17879	Heat shock 70 kDa protein 1B	891.74	-0.487
P28652	Calcium/calmodulin-dependent protein kinase type II subunit beta	1850.3	-0.492
Q61696	Heat shock 70 kDa protein 1A	891.74	-0.492
P18872	Guanine nucleotide-binding protein G(o) subunit alpha	2986.96	-0.527
Q03265	ATP synthase subunit alpha, mitochondrial	2101.69	-0.533
Q62277	Synaptophysin	517.81	-0.543
P04370	Myelin basic protein	9022.31	-0.549
Q9Z1W8	Potassium-transporting ATPase alpha chain 2	514.97	-0.554
Q9WV27	Sodium/potassium-transporting ATPase subunit alpha-4	531.64	-0.577
P53657	Pyruvate kinase PKLR	382.02	-0.583
P10126	Elongation factor 1-alpha 1	355.16	-0.607
P52480	Pyruvate kinase PKM	5072.32	-0.613
P08249	Malate dehydrogenase, mitochondrial	3024.44	-0.625
O08599	Syntaxin-binding protein 1	1908.06	-0.644
Q68FD5	Clathrin heavy chain 1	227.48	-0.651
Q9D6P8	Calmodulin-like protein 3	89.23	-0.664
P05202	Aspartate aminotransferase, mitochondrial	883.71	-0.719
P08553	Neurofilament medium polypeptide	365.1	-0.719
P0DP27	Calmodulin-2	1448.27	-0.733
P16627	Heat shock 70 kDa protein 1-like	864.62	-0.733
Q64332	Synapsin-2	356.6	-0.733
P0DP26	Calmodulin-1	1448.27	-0.741
P0DP28	Calmodulin-3	1448.27	-0.741
P60879	Synaptosomal-associated protein 25	197.72	-0.748
P62962	Profilin-1	1570.27	-0.756
P46660	Alpha-internexin	52.44	-0.779
Q99PT1	Rho GDP-dissociation inhibitor 1	335.24	-0.819

O88935	Synapsin-1	752.24	-0.827
P17183	Gamma-enolase	3347.39	-0.844
P16858	Glyceraldehyde-3-phosphate dehydrogenase	13052.28	-0.844
P18760	Cofilin-1	1063.08	-0.852
Q04447	Creatine kinase B-type	3079.53	-0.869
P17751	Triosephosphate isomerase	1422.35	-0.869
P68033	Actin, alpha cardiac muscle 1	24755.44	-0.878
Q922F4	Tubulin beta-6 chain	14837.39	-0.887
P21550	Beta-enolase	1943.89	-0.905
Q8BFZ3	Beta-actin-like protein 2	7162.73	-0.923
P68368	Tubulin alpha-4A chain	14150.28	-0.923
P63268	Actin, gamma-enteric smooth muscle	24558.29	-0.932
Q3TXS7	26S proteasome non-ATPase regulatory subunit 1	114.46	Control
Q9R0Q6	Actin-related protein 2/3 complex subunit 1A	70.32	Control
Q99JY9	Actin-related protein 3	184.91	Control
Q9QXN3	Activating signal cointegrator 1	64.68	Control
P40124	Adenylyl cyclase-associated protein 1	340.87	Control
E9Q394	A-kinase anchor protein 13	49.13	Control
Q9JII6	Aldo-keto reductase family 1 member A1	122.11	Control
P84091	AP-2 complex subunit mu	138.32	Control
Q91V80	Apolipoprotein F	151.7	Control
O88879	Apoptotic protease-activating factor 1	85	Control
P39654	Arachidonate 15-lipoxygenase	45.59	Control
P98203	Armadillo repeat protein deleted in velo-cardio-facial syndrome homolog	51.81	Control
Q9DBR3	Armadillo repeat-containing protein 8	35.27	Control
Q91YH5	Atlastin-3	105.62	Control
Q9CQQ7	ATP synthase F(0) complex subunit B1, mitochondrial	126.25	Control
P03930	ATP synthase protein 8	681.06	Control
Q9D3D9	ATP synthase subunit delta, mitochondrial	366.15	Control
E9PX95	ATP-binding cassette sub-family A member 17	41.04	Control
B5X0E4	ATP-binding cassette sub-family B member 5	87.08	Control
Q9DBI2	Bardet-Biedl syndrome 10 protein homolog	54.26	Control
Q8CDE2	Calicin	49.27	Control

Q5PR69	Cancer-related regulator of actin dynamics	43.25	Control
Q9CTG6	Cation-transporting ATPase 13A2	70.86	Control
Q5PR68	Centrosomal protein of 112 kDa	47.55	Control
Q3UPP8	Centrosomal protein of 63 kDa	35.86	Control
Q9Z0X4	cGMP-inhibited 3',5'-cyclic phosphodiesterase A	25.5	Control
Q61548	Clathrin coat assembly protein AP180	76.8	Control
Q8CDV0	Coiled-coil domain-containing protein 178	42.91	Control
Q2UY11	Collagen alpha-1(XXVIII) chain	102.74	Control
Q6DFV1	Condensin-2 complex subunit G2	221.95	Control
Q6ZQ38	Cullin-associated NEDD8-dissociated protein 1	46.13	Control
Q62425	Cytochrome c oxidase subunit NDUFA4	1346.01	Control
Q8BPN8	DmX-like protein 2	27.86	Control
Q8BHK9	DNA excision repair protein ERCC-6-like	16.41	Control
P33611	DNA polymerase alpha subunit B	77.5	Control
P70388	DNA repair protein RAD50	47.24	Control
Q8C7R7	DNA-binding protein RFX6	56.61	Control
Q3V0Q1	Dynein heavy chain 12, axonemal	42.8	Control
Q91XQ0	Dynein heavy chain 8, axonemal	23.7	Control
Q6ZQM0	E3 ubiquitin-protein ligase rififylin	69.42	Control
Q3TGW2	Endonuclease/exonuclease/phosphatase family domain-containing protein 1	90.5	Control
P08113	Endoplasmin	28.95	Control
Q8R418	Endoribonuclease Dicer	45.65	Control
Q3TDN2	FAS-associated factor 2	115.28	Control
Q922J9	Fatty acyl-CoA reductase 1	64.67	Control
Q80ZA4	Fibrocystin-L	23.87	Control
Q8CI03	FLYWCH-type zinc finger-containing protein 1	142.23	Control
P49772	Fms-related tyrosine kinase 3 ligand	100.11	Control
Q8K0C9	GDP-mannose 4,6 dehydratase	51.77	Control
P97324	Glucose-6-phosphate 1-dehydrogenase 2	38.33	Control
Q9D4P7	Glutathione S-transferase theta-4	127.3	Control
Q8CI94	Glycogen phosphorylase, brain form	54.74	Control
Q9ET01	Glycogen phosphorylase, liver form	49.53	Control
Q9WUB3	Glycogen phosphorylase, muscle form	33.78	Control

Q3UFB7	High affinity nerve growth factor receptor	46.22	Control
Q8C2B3	Histone deacetylase 7	46.29	Control
Q63ZW7	InaD-like protein	108.24	Control
P56477	Interferon regulatory factor 5	136.19	Control
Q6IME9	Keratin, type II cytoskeletal 72	52.82	Control
P28738	Kinesin heavy chain isoform 5C	49.49	Control
Q9QXL2	Kinesin-like protein KIF21A	70.96	Control
Q3URE9	Leucine-rich repeat and immunoglobulin-like domain-containing nogo receptor-interacting protein 2	106.78	Control
Q80U28	MAP kinase-activating death domain protein	82.2	Control
P53349	Mitogen-activated protein kinase kinase kinase 1	42.29	Control
Q99LC3	NADH dehydrogenase [ubiquinone] 1 alpha subcomplex subunit 10, mitochondrial	590.31	Control
Q9D6J5	NADH dehydrogenase [ubiquinone] 1 beta subcomplex subunit 8, mitochondrial	74.34	Control
Q810U3	Neurofascin	81.34	Control
Q8CH77	Neuron navigator 1	37.69	Control
Q6DFV7	Nuclear receptor coactivator 7	55.17	Control
Q8K4K6	Pantothenate kinase 1	56.14	Control
Q8R1G6	PDZ and LIM domain protein 2	54.81	Control
Q8CGT6	Piwi-like protein 4	77.12	Control
Q7TQ62	Podocan	87.39	Control
Q91Z31	Polypyrimidine tract-binding protein 2	53.52	Control
Q99MQ1	Protein bicaudal C homolog 1	60.29	Control
P27773	Protein disulfide-isomerase A3	57.17	Control
Q9DAI6	Protein FAM135B	46.17	Control
E9Q8I9	Protein furry homolog	49.48	Control
Q61644	Protein kinase C and casein kinase substrate in neurons protein 1	140.75	Control
Q8R1F1	Protein Niban 2	87.89	Control
E5FYH1	Protein TOPAZ1	48.39	Control
Q8K3V4	Protein-arginine deiminase type-6	54.78	Control
Q91Y02	Protocadherin beta-18	65	Control
P35486	Pyruvate dehydrogenase E1 component subunit alpha, somatic form, mitochondrial	75.76	Control
Q8VCD6	Receptor expression-enhancing protein 2	103.82	Control
Q62132	Receptor-type tyrosine-protein phosphatase R	43.05	Control

B9EKR1	Receptor-type tyrosine-protein phosphatase zeta	21.41	Control
Q8K0T0	Reticulon-1	68.24	Control
Q9ES97	Reticulon-3	69.89	Control
Q80U35	Rho guanine nucleotide exchange factor 17	48.63	Control
Q9D3G9	Rho-related GTP-binding protein RhoH	86.75	Control
Q3UZ01	RNA-binding region-containing protein 3	100.41	Control
P60330	Separin	62.04	Control
Q91ZR4	Serine/threonine-protein kinase Nek8	39.5	Control
Q9JK88	Serpin I2	57.22	Control
Q60665	Ski-like protein	41.91	Control
Q8K596	Sodium/calcium exchanger 2	64.72	Control
Q8K078	Solute carrier organic anion transporter family member 4A1	58.66	Control
Q9D3S3	Sorting nexin-29	26.68	Control
Q5U4C3	Splicing factor, arginine/serine-rich 19	29.48	Control
F6XZJ7	Sterile alpha motif domain-containing protein 15	44.9	Control
P83093	Stromal interaction molecule 2	48.68	Control
Q9WUM5	Succinate--CoA ligase [ADP/GDP-forming] subunit alpha, mitochondrial	340.57	Control
Q9Z2I9	Succinate--CoA ligase [ADP-forming] subunit beta, mitochondrial	48.27	Control
O55100	Synaptogyrin-1	262.69	Control
Q8CHC4	Synaptojanin-1	95.51	Control
P80316	T-complex protein 1 subunit epsilon	200.72	Control
P42932	T-complex protein 1 subunit theta	149.24	Control
Q80W22	Threonine synthase-like 2	96.5	Control
Q9Z1T2	Thrombospondin-4	52.59	Control
Q61286	Transcription factor 12	98.9	Control
P42669	Transcriptional activator protein Pur-alpha	126.95	Control
Q9R1Q8	Transgelin-3	138.09	Control
Q7TQI3	Ubiquitin thioesterase OTUB1	99.66	Control
Q9D906	Ubiquitin-like modifier-activating enzyme ATG7	56.75	Control
P40336	Vacuolar protein sorting-associated protein 26A	139.42	Control
P29788	Vitronectin	55.89	Control
Q9Z1B3	1-phosphatidylinositol 4,5-bisphosphate phosphodiesterase beta-1	41.48	10 mg/L
Q60597	2-oxoglutarate dehydrogenase, mitochondrial	92.99	10 mg/L

P61922	4-aminobutyrate aminotransferase, mitochondrial	573.78	10 mg/L
P10852	4F2 cell-surface antigen heavy chain	132.09	10 mg/L
Q5SSL4	Active breakpoint cluster region-related protein	51.4	10 mg/L
P31786	Acyl-CoA-binding protein	1471.59	10 mg/L
P84078	ADP-ribosylation factor 1	1615.26	10 mg/L
Q8BSL7	ADP-ribosylation factor 2	1134.59	10 mg/L
P61205	ADP-ribosylation factor 3	1615.26	10 mg/L
P61750	ADP-ribosylation factor 4	815.33	10 mg/L
P84084	ADP-ribosylation factor 5	815.33	10 mg/L
Q80Y20	Alkylated DNA repair protein alkB homolog 8	129.16	10 mg/L
Q9QYC0	Alpha-adducin	480.63	10 mg/L
Q7TQF7	Amphiphysin	81.33	10 mg/L
Q8C6Y6	Ankyrin repeat and SOCS box protein 14	57.7	10 mg/L
O35643	AP-1 complex subunit beta-1	60.21	10 mg/L
Q9DBG3	AP-2 complex subunit beta	110.45	10 mg/L
P06728	Apolipoprotein A-IV	180.65	10 mg/L
Q99KN1	Arrestin domain-containing protein 1	175.26	10 mg/L
Q9DCX2	ATP synthase subunit d, mitochondrial	407.79	10 mg/L
P97450	ATP synthase-coupling factor 6, mitochondrial	785.56	10 mg/L
Q9DC29	ATP-binding cassette sub-family B member 6, mitochondrial	32.46	10 mg/L
Q99PU8	ATP-dependent RNA helicase DHX30	149.18	10 mg/L
Q80XK6	Autophagy-related protein 2 homolog B	56.63	10 mg/L
Q9Z2H5	Band 4.1-like protein 1	55.35	10 mg/L
Q9WV92	Band 4.1-like protein 3	91.02	10 mg/L
Q9QYB8	Beta-adducin	84.36	10 mg/L
Q8BKX1	Brain-specific angiogenesis inhibitor 1-associated protein 2	130.66	10 mg/L
Q61361	Brevican core protein	68.86	10 mg/L
Q9R1S8	Calpain-7	68.21	10 mg/L
Q65CL1	Catenin alpha-3	54.03	10 mg/L
P35762	CD81 antigen	627.76	10 mg/L
Q99N28	Cell adhesion molecule 3	230.14	10 mg/L
Q6A065	Centrosomal protein of 170 kDa	88.12	10 mg/L
Q9EPU4	Cleavage and polyadenylation specificity factor subunit 1	137.64	10 mg/L

Q8CDI7	Coiled-coil domain-containing protein 150	73.6	10 mg/L
P63040	Complexin-1	31.93	10 mg/L
P84086	Complexin-2	429.62	10 mg/L
Q8CI04	Conserved oligomeric Golgi complex subunit 3	29.61	10 mg/L
Q9DB77	Cytochrome b-c1 complex subunit 2, mitochondrial	430.39	10 mg/L
P19536	Cytochrome c oxidase subunit 5B, mitochondrial	392.36	10 mg/L
P56391	Cytochrome c oxidase subunit 6B1	192.35	10 mg/L
P48771	Cytochrome c oxidase subunit 7A2, mitochondrial	514.4	10 mg/L
P62897	Cytochrome c, somatic	498.73	10 mg/L
Q8C4S8	DENN domain-containing protein 2A	64.83	10 mg/L
Q9EQF6	Dihydropyrimidinase-related protein 5	70.73	10 mg/L
Q811D0	Disks large homolog 1	78.4	10 mg/L
Q91XM9	Disks large homolog 2	98.04	10 mg/L
Q62108	Disks large homolog 4	206.56	10 mg/L
Q6PFD5	Disks large-associated protein 3	52.24	10 mg/L
Q3UYV8	Dynein assembly factor 3, axonemal	78.6	10 mg/L
Q8BFR5	Elongation factor Tu, mitochondrial	111.39	10 mg/L
Q9DCS3	Enoyl-[acyl-carrier-protein] reductase, mitochondrial	119.84	10 mg/L
Q0VAV2	Exophilin-5	38.17	10 mg/L
Q9ERK4	Exportin-2	81.71	10 mg/L
P47754	F-actin-capping protein subunit alpha-2	227.89	10 mg/L
Q80X90	Filamin-B	32.25	10 mg/L
P97807	Fumarate hydratase, mitochondrial	153.96	10 mg/L
D3Z7P3	Glutaminase kidney isoform, mitochondrial	99.06	10 mg/L
P19157	Glutathione S-transferase P 1	1099.34	10 mg/L
P46425	Glutathione S-transferase P 2	495.07	10 mg/L
Q61316	Heat shock 70 kDa protein 4	102.54	10 mg/L
P48722	Heat shock 70 kDa protein 4L	93.19	10 mg/L
Q61699	Heat shock protein 105 kDa	59.3	10 mg/L
Q9WV07	Hydroperoxide isomerase ALOXE3	59.28	10 mg/L
Q3KNY0	Immunoglobulin-like and fibronectin type III domain-containing protein 1	29.85	10 mg/L
Q571I4	Inactive tyrosine-protein kinase PRAG1	58.94	10 mg/L
Q80V86	Integrator complex subunit 8	71.24	10 mg/L

Q60625	Intercellular adhesion molecule 5	48.95	10 mg/L
Q9D8C4	Interferon-induced 35 kDa protein homolog	307.48	10 mg/L
Q9QZ85	Interferon-inducible GTPase 1	58.34	10 mg/L
Q62406	Interleukin-1 receptor-associated kinase 1	142.9	10 mg/L
P11369	LINE-1 retrotransposable element ORF2 protein	40.09	10 mg/L
Q9JI18	Low-density lipoprotein receptor-related protein 1B	39.31	10 mg/L
Q9JJ78	Lymphokine-activated killer T-cell-originated protein kinase	69.55	10 mg/L
Q9QYR6	Microtubule-associated protein 1A	42.54	10 mg/L
Q7TSJ2	Microtubule-associated protein 6	116.38	10 mg/L
Q9D6M3	Mitochondrial glutamate carrier 1	1913.94	10 mg/L
Q9DB41	Mitochondrial glutamate carrier 2	264.97	10 mg/L
Q63844	Mitogen-activated protein kinase 3	130.87	10 mg/L
O08539	Myc box-dependent-interacting protein 1	320.05	10 mg/L
Q61885	Myelin-oligodendrocyte glycoprotein	287.13	10 mg/L
Q9D6J6	NADH dehydrogenase [ubiquinone] flavoprotein 2, mitochondrial	554.17	10 mg/L
P52503	NADH dehydrogenase [ubiquinone] iron-sulfur protein 6, mitochondrial	194.46	10 mg/L
Q91VD9	NADH-ubiquinone oxidoreductase 75 kDa subunit, mitochondrial	303.78	10 mg/L
Q6GQX2	Nck-associated protein 5-like	147.69	10 mg/L
Q8R007	Nectin-4	72.22	10 mg/L
P70211	Netrin receptor DCC	45.19	10 mg/L
P06837	Neuromodulin	347.57	10 mg/L
P35802	Neuronal membrane glycoprotein M6-a	67.63	10 mg/L
Q9QXX8	Nuclear fragile X mental retardation-interacting protein 1	98.96	10 mg/L
Q61937	Nucleophosmin	82.67	10 mg/L
O54998	Peptidyl-prolyl cis-trans isomerase FKBP7	99.86	10 mg/L
P35700	Peroxiredoxin-1	796.59	10 mg/L
O08807	Peroxiredoxin-4	70.37	10 mg/L
Q5BL07	Peroxisome biogenesis factor 1	140.96	10 mg/L
Q91YL7	PGAP2-interacting protein	52.95	10 mg/L
O70250	Phosphoglycerate mutase 2	112.61	10 mg/L
P98199	Phospholipid-transporting ATPase ID	48.24	10 mg/L
Q8CDG1	Piwi-like protein 2	131.71	10 mg/L
P0CG49	Polyubiquitin-B	1318.22	10 mg/L

P0CG50	Polyubiquitin-C	1318.22	10 mg/L
P67778	Prohibitin	102.37	10 mg/L
O35129	Prohibitin-2	402.09	10 mg/L
Q9QXV0	ProSAAS	113.13	10 mg/L
Q61207	Prosaposin	74.57	10 mg/L
O55125	Protein NipSnap homolog 1	173.16	10 mg/L
Q9CU24	Protein THEMIS3	47.42	10 mg/L
P35294	Ras-related protein Rab-19	293.2	10 mg/L
P24549	Retinal dehydrogenase 1	132.8	10 mg/L
Q8BRH3	Rho GTPase-activating protein 19	82.39	10 mg/L
Q8BWA8	Rho guanine nucleotide exchange factor 19	263.26	10 mg/L
Q9JLC8	Sacsin	79.77	10 mg/L
Q9CZC8	Secernin-1	250.9	10 mg/L
Q8C650	Septin-10	66.2	10 mg/L
Q8C1B7	Septin-11	109.63	10 mg/L
Q9DA97	Septin-14	66.2	10 mg/L
Q9R1T4	Septin-6	291.67	10 mg/L
B2RXR6	Serine/threonine-protein phosphatase 6 regulatory ankyrin repeat subunit B	116.3	10 mg/L
Q4VA53	Sister chromatid cohesion protein PDS5 homolog B	44.45	10 mg/L
Q3UHA3	Spatacsin	34.61	10 mg/L
P52019	Squalene monooxygenase	139.92	10 mg/L
P61264	Syntaxin-1B	374.9	10 mg/L
Q71LX4	Talin-2	48.84	10 mg/L
Q3UR70	Transforming growth factor-beta receptor-associated protein 1	101.94	10 mg/L
Q00993	Tyrosine-protein kinase receptor UFO	51.64	10 mg/L
P56399	Ubiquitin carboxyl-terminal hydrolase 5	68.64	10 mg/L
P62983	Ubiquitin-40S ribosomal protein S27a	1318.22	10 mg/L
P62984	Ubiquitin-60S ribosomal protein L40	1318.22	10 mg/L
Q9DBP5	UMP-CMP kinase	91.98	10 mg/L
P63024	Vesicle-associated membrane protein 3	40.24	10 mg/L
P62761	Visinin-like protein 1	134.82	10 mg/L
Q60931	Voltage-dependent anion-selective channel protein 3	102.28	10 mg/L
P51863	V-type proton ATPase subunit d 1	159.48	10 mg/L

P50518	V-type proton ATPase subunit E 1	302.13	10 mg/L
Q8BVE3	V-type proton ATPase subunit H	172.23	10 mg/L

[a]Uniprot accession ID retrieved from uniport.org database; Negative values of fold change mean down-regulated proteins; 10 mg/L or Control in fold change column means that protein was exclusively found in the respective experimental.

Supplementary table 3. Identified proteins with expression significantly altered in the hippocampus of mice in 50 mg/L vs. control group.

Accession Id[a]	Description	PLGS Score	Fold Change
Q8BZQ7	Anaphase-promoting complex subunit 2	49.72	8.41
Q3TGW2	Endonuclease/exonuclease/phosphatase family domain-containing protein 1	90.5	4.18
Q64467	Glyceraldehyde-3-phosphate dehydrogenase, testis-specific	103.28	2.69
Q9DB05	Alpha-soluble NSF attachment protein	54.03	2.27
P15626	Glutathione S-transferase Mu 2	97.07	2.16
A2AQ07	Tubulin beta-1 chain	527.66	2.08
Q80W21	Glutathione S-transferase Mu 7	97.07	2.03
Q9Z1W8	Potassium-transporting ATPase alpha chain 2	514.97	2.01
Q64436	Potassium-transporting ATPase alpha chain 1	110.77	1.97
P02104	Hemoglobin subunit epsilon-Y2	1972	1.88
P26883	Peptidyl-prolyl cis-trans isomerase FKBP1A	1709.6	1.88
P13595	Neural cell adhesion molecule 1	40.83	1.84
P09041	Phosphoglycerate kinase 2	133.46	1.84
Q8BFZ3	Beta-actin-like protein 2	7162.7	1.80
P48774	Glutathione S-transferase Mu 5	47.83	1.79
P0DP26	Calmodulin-1	1448.3	1.77
Q7TMM9	Tubulin beta-2A chain	37521	1.77
O55131	Septin-7	270.57	1.73
Q922F4	Tubulin beta-6 chain	14837	1.73
Q9CQN1	Heat shock protein 75 kDa, mitochondrial	242.62	1.68

P02088	Hemoglobin subunit beta-1	3543.4	1.67
Q64525	Histone H2B type 2-B	1013.8	1.65
Q64524	Histone H2B type 2-E	852.51	1.65
P99024	Tubulin beta-5 chain	35888	1.65
P70696	Histone H2B type 1-A	711.41	1.63
P10853	Histone H2B type 1-F/J/L	1013.8	1.63
Q64475	Histone H2B type 1-B	1013.8	1.60
Q6ZWY9	Histone H2B type 1-C/E/G	1013.8	1.60
Q8CGP1	Histone H2B type 1-K	1013.8	1.57
P62806	Histone H4	1669.8	1.54
P68369	Tubulin alpha-1A chain	12360	1.52
P02089	Hemoglobin subunit beta-2	1972	1.51
P17751	Triosephosphate isomerase	1422.4	1.49
P68373	Tubulin alpha-1C chain	11309	1.49
P16858	Glyceraldehyde-3-phosphate dehydrogenase	13052	1.48
P08249	Malate dehydrogenase, mitochondrial	3024.4	1.48
P11798	Calcium/calmodulin-dependent protein kinase type II subunit alpha	4430.8	1.46
P50516	V-type proton ATPase catalytic subunit A	277.79	1.46
P63268	Actin, gamma-enteric smooth muscle	24558	1.45
P51881	ADP/ATP translocase 2	102.17	1.45
Q9JJZ2	Tubulin alpha-8 chain	4374.6	1.43
P30275	Creatine kinase U-type, mitochondrial	521.45	1.40
P29387	Guanine nucleotide-binding protein subunit beta-4	984.78	1.40
P07901	Heat shock protein HSP 90-alpha	283.32	1.38
Q9CZU6	Citrate synthase, mitochondrial	136.89	1.36
Q61011	Guanine nucleotide-binding protein G(I)/G(S)/G(T) subunit beta-3	150.23	1.36
P84091	AP-2 complex subunit mu	138.32	1.35
P68134	Actin, alpha skeletal muscle	24717	1.34
P62737	Actin, aortic smooth muscle	24552	1.34
O55042	Alpha-synuclein	477.8	1.34
Q9D6P8	Calmodulin-like protein 3	89.23	1.34
P07724	Serum albumin	102.93	1.34
Q64332	Synapsin-2	356.6	1.34

P68033	Actin, alpha cardiac muscle 1	24755	1.32
P48962	ADP/ATP translocase 1	173.37	1.31
P14094	Sodium/potassium-transporting ATPase subunit beta-1	604.37	1.31
P28663	Beta-soluble NSF attachment protein	133.71	1.30
P06745	Glucose-6-phosphate isomerase	613.13	1.30
P62880	Guanine nucleotide-binding protein G(I)/G(S)/G(T) subunit beta-2	1227.2	1.28
P47857	ATP-dependent 6-phosphofructokinase, muscle type	66.63	1.26
P17182	Alpha-enolase	4175.8	1.25
Q64521	Glycerol-3-phosphate dehydrogenase, mitochondrial	81.8	1.25
P70404	Isocitrate dehydrogenase [NAD] subunit gamma 1, mitochondrial	196.92	1.25
P70296	Phosphatidylethanolamine-binding protein 1	944.72	1.25
Q6PIC6	Sodium/potassium-transporting ATPase subunit alpha-3	1247.9	1.25
Q91ZZ3	Beta-synuclein	76.97	1.23
P43006	Excitatory amino acid transporter 2	262.57	1.23
P26443	Glutamate dehydrogenase 1, mitochondrial	717.95	1.23
P01942	Hemoglobin subunit alpha	2208.1	1.23
Q9Z0E0	Neurochondrin	107.25	1.23
P63328	Serine/threonine-protein phosphatase 2B catalytic subunit alpha isoform	209.5	1.23
Q6PIE5	Sodium/potassium-transporting ATPase subunit alpha-2	1008.5	1.23
Q9WV27	Sodium/potassium-transporting ATPase subunit alpha-4	531.64	1.23
Q03265	ATP synthase subunit alpha, mitochondrial	2101.7	1.22
P39053	Dynamin-1	4943.2	1.22
P14152	Malate dehydrogenase, cytoplasmic	2371.9	1.22
P62874	Guanine nucleotide-binding protein G(I)/G(S)/G(T) subunit beta-1	996.97	1.21
Q8VDN2	Sodium/potassium-transporting ATPase subunit alpha-1	778.3	1.21
Q9DB20	ATP synthase subunit O, mitochondrial	1284.3	1.20
P0DP27	Calmodulin-2	1448.3	1.20
P0DP28	Calmodulin-3	1448.3	1.20
O08599	Syntaxin-binding protein 1	1908.1	1.20
Q8BZ98	Dynamin-3	81.67	1.19
P10126	Elongation factor 1-alpha 1	355.16	1.19
P05063	Fructose-bisphosphate aldolase C	782.97	1.19
P31001	Desmin	114.92	1.17

Q64478	Histone H2B type 1-H	1013.8	1.17
P10854	Histone H2B type 1-M	1013.8	1.17
Q8CGP2	Histone H2B type 1-P	1013.8	1.17
P05213	Tubulin alpha-1B chain	12033	1.17
P05201	Aspartate aminotransferase, cytoplasmic	401.64	1.16
P21550	Beta-enolase	1943.9	1.16
Q9D2U9	Histone H2B type 3-A	852.51	1.16
P50396	Rab GDP dissociation inhibitor alpha	386.95	1.16
Q9CZ13	Cytochrome b-c1 complex subunit 1, mitochondrial	232.11	1.15
C0HKE7	Histone H2A type 1-N	1343.4	1.15
Q8CGP0	Histone H2B type 3-B	852.51	1.15
P05214	Tubulin alpha-3 chain	7666.1	1.15
P68368	Tubulin alpha-4A chain	14150	1.15
Q9CWF2	Tubulin beta-2B chain	37032	1.15
P46460	Vesicle-fusing ATPase	225.46	1.15
P39054	Dynamin-2	80.91	1.14
P08553	Neurofilament medium polypeptide	365.1	1.14
P52480	Pyruvate kinase PKM	5072.3	1.14
O88935	Synapsin-1	752.24	1.14
P68372	Tubulin beta-4B chain	28844	1.14
Q60932	Voltage-dependent anion-selective channel protein 1	1508.7	1.14
Q68FD5	Clathrin heavy chain 1	227.48	1.13
P08551	Neurofilament light polypeptide	57.38	1.13
P46096	Synaptotagmin-1	213.16	1.13
Q9ERD7	Tubulin beta-3 chain	25756	1.13
Q6PHZ2	Calcium/calmodulin-dependent protein kinase type II subunit delta	1299.8	1.12
P62814	V-type proton ATPase subunit B, brain isoform	95.93	1.12
P17183	Gamma-enolase	3347.4	1.11
P62631	Elongation factor 1-alpha 2	167.42	1.09
P99029	Peroxiredoxin-5, mitochondrial	1039.1	1.09
P05202	Aspartate aminotransferase, mitochondrial	883.71	1.08
P05064	Fructose-bisphosphate aldolase A	3093.5	1.08
P16546	Spectrin alpha chain, non-erythrocytic 1	133.67	1.08

P28652	Calcium/calmodulin-dependent protein kinase type II subunit beta	1850.3	1.07
P63101	14-3-3 protein zeta/delta	4286.1	1.05
Q62420	Endophilin-A1	473.69	-0.52
Q8CGK7	Guanine nucleotide-binding protein G(olf) subunit alpha	1628.3	-0.55
Q62419	Endophilin-A2	247.38	-0.57
P20801	Troponin C, skeletal muscle	394.5	-0.57
B2RSH2	Guanine nucleotide-binding protein G(i) subunit alpha-1	1623.5	-0.58
Q9DC51	Guanine nucleotide-binding protein G(i) subunit alpha	1623.5	-0.58
P08752	Guanine nucleotide-binding protein G(i) subunit alpha-2	1623.5	-0.58
P17156	Heat shock-related 70 kDa protein 2	933.05	-0.66
Q91XV3	Brain acid soluble protein 1	436.33	-0.72
P63044	Vesicle-associated membrane protein 2	565.75	-0.73
P19783	Cytochrome c oxidase subunit 4 isoform 1, mitochondrial	321.26	-0.78
P16330	2',3'-cyclic-nucleotide 3'-phosphodiesterase	887.7	-0.83
P46097	Synaptotagmin-2	62.99	-0.84
P60202	Myelin proteolipid protein	5128.6	-0.86
P01831	Thy-1 membrane glycoprotein	202.4	-0.86
P16627	Heat shock 70 kDa protein 1-like	864.62	-0.88
Q62277	Synaptophysin	517.81	-0.88
P63017	Heat shock cognate 71 kDa protein	2484.2	-0.90
P04370	Myelin basic protein	9022.3	-0.90
O08553	Dihydropyrimidinase-related protein 2	6913.4	-0.91
P18872	Guanine nucleotide-binding protein G(o) subunit alpha	2987	-0.91
P97427	Dihydropyrimidinase-related protein 1	1567.8	-0.94
P63260	Actin, cytoplasmic 2	32990	-0.97
Q3TXS7	26S proteasome non-ATPase regulatory subunit 1	114.46	Control
Q9QXN3	Activating signal cointegrator 1	64.68	Control
E9Q394	A-kinase anchor protein 13	49.13	Control
Q9JII6	Aldo-keto reductase family 1 member A1	122.11	Control
Q91V80	Apolipoprotein F	151.7	Control
O88879	Apoptotic protease-activating factor 1	85	Control
P39654	Arachidonate 15-lipoxygenase	45.59	Control
P98203	Armadillo repeat protein deleted in velo-cardio-facial syndrome homolog	51.81	Control

Q9DBR3	Armadillo repeat-containing protein 8	35.27	Control
Q91YH5	Atlastin-3	105.62	Control
Q9CQQ7	ATP synthase F(0) complex subunit B1, mitochondrial	126.25	Control
P03930	ATP synthase protein 8	681.06	Control
Q9D3D9	ATP synthase subunit delta, mitochondrial	366.15	Control
Q91VR2	ATP synthase subunit gamma, mitochondrial	148.77	Control
E9PX95	ATP-binding cassette sub-family A member 17	41.04	Control
B5X0E4	ATP-binding cassette sub-family B member 5	87.08	Control
Q5PR69	Cancer-related regulator of actin dynamics	43.25	Control
Q9CTG6	Cation-transporting ATPase 13A2	70.86	Control
Q5PR68	Centrosomal protein of 112 kDa	47.55	Control
Q3UPP8	Centrosomal protein of 63 kDa	35.86	Control
Q9Z0X4	cGMP-inhibited 3',5'-cyclic phosphodiesterase A	25.5	Control
Q6ZPV2	Chromatin-remodeling ATPase INO80	39.29	Control
Q61548	Clathrin coat assembly protein AP180	76.8	Control
Q8CDV0	Coiled-coil domain-containing protein 178	42.91	Control
Q2UY11	Collagen alpha-1(XXVIII) chain	102.74	Control
Q6DFV1	Condensin-2 complex subunit G2	221.95	Control
Q8BPN8	DmX-like protein 2	27.86	Control
Q8BHK9	DNA excision repair protein ERCC-6-like	16.41	Control
P33611	DNA polymerase alpha subunit B	77.5	Control
P70388	DNA repair protein RAD50	47.24	Control
Q8C7R7	DNA-binding protein RFX6	56.61	Control
Q3V0Q1	Dynein heavy chain 12, axonemal	42.8	Control
Q91XQ0	Dynein heavy chain 8, axonemal	23.7	Control
Q6ZQM0	E3 ubiquitin-protein ligase rififylin	69.42	Control
Q5SQM0	Echinoderm microtubule-associated protein-like 6	49.6	Control
P08113	Endoplasmin	28.95	Control
Q8R418	Endoribonuclease Dicer	45.65	Control
Q3TDN2	FAS-associated factor 2	115.28	Control
Q922J9	Fatty acyl-CoA reductase 1	64.67	Control
Q80ZA4	Fibrocystin-L	23.87	Control
Q8CI03	FLYWCH-type zinc finger-containing protein 1	142.23	Control

P49772	Fms-related tyrosine kinase 3 ligand	100.11	Control
Q8K0C9	GDP-mannose 4,6 dehydratase	51.77	Control
P97324	Glucose-6-phosphate 1-dehydrogenase 2	38.33	Control
Q9D4P7	Glutathione S-transferase theta-4	127.3	Control
Q3UFB7	High affinity nerve growth factor receptor	46.22	Control
Q8C2B3	Histone deacetylase 7	46.29	Control
Q63ZW7	InaD-like protein	108.24	Control
P56477	Interferon regulatory factor 5	136.19	Control
A2CG49	Kalirin	47.52	Control
Q6IME9	Keratin, type II cytoskeletal 72	52.82	Control
P28738	Kinesin heavy chain isoform 5C	49.49	Control
Q3URE9	Leucine-rich repeat and immunoglobulin-like domain-containing nogo receptor-interacting protein 2	106.78	Control
P51885	Lumican	87.64	Control
Q80U28	MAP kinase-activating death domain protein	82.2	Control
P53349	Mitogen-activated protein kinase kinase kinase 1	42.29	Control
Q9D6J5	NADH dehydrogenase [ubiquinone] 1 beta subcomplex subunit 8, mitochondrial	74.34	Control
Q9DCT2	NADH dehydrogenase [ubiquinone] iron-sulfur protein 3, mitochondrial	105.89	Control
Q8CH77	Neuron navigator 1	37.69	Control
Q6DFV7	Nuclear receptor coactivator 7	55.17	Control
Q8K4K6	Pantothenate kinase 1	56.14	Control
Q8R1G6	PDZ and LIM domain protein 2	54.81	Control
O70167	Phosphatidylinositol 4-phosphate 3-kinase C2 domain-containing subunit gamma	116.13	Control
Q8CGT6	Piwi-like protein 4	77.12	Control
Q7TQ62	Podocan	87.39	Control
Q91Z31	Polypyrimidine tract-binding protein 2	53.52	Control
Q99MQ1	Protein bicaudal C homolog 1	60.29	Control
P27773	Protein disulfide-isomerase A3	57.17	Control
Q9DAI6	Protein FAM135B	46.17	Control
E9Q8I9	Protein furry homolog	49.48	Control
Q61644	Protein kinase C and casein kinase substrate in neurons protein 1	140.75	Control
Q8R1F1	Protein Niban 2	87.89	Control
Q8K3V4	Protein-arginine deiminase type-6	54.78	Control
Q91Y02	Protocadherin beta-18	65	Control

Q8VCD6	Receptor expression-enhancing protein 2	103.82	Control
Q62132	Receptor-type tyrosine-protein phosphatase R	43.05	Control
B9EKR1	Receptor-type tyrosine-protein phosphatase zeta	21.41	Control
Q8K0T0	Reticulon-1	68.24	Control
Q80U35	Rho guanine nucleotide exchange factor 17	48.63	Control
Q9D3G9	Rho-related GTP-binding protein RhoH	86.75	Control
Q3UZ01	RNA-binding region-containing protein 3	100.41	Control
P60330	Separin	62.04	Control
Q91ZR4	Serine/threonine-protein kinase Nek8	39.5	Control
Q9JK88	Serpin I2	57.22	Control
Q60665	Ski-like protein	41.91	Control
Q8K596	Sodium/calcium exchanger 2	64.72	Control
Q8K078	Solute carrier organic anion transporter family member 4A1	58.66	Control
Q9D3S3	Sorting nexin-29	26.68	Control
A0AUV4	Sperm motility kinase Y	79.3	Control
Q5U4C3	Splicing factor, arginine/serine-rich 19	29.48	Control
F6XZJ7	Sterile alpha motif domain-containing protein 15	44.9	Control
P83093	Stromal interaction molecule 2	48.68	Control
Q9WUM5	Succinate--CoA ligase [ADP/GDP-forming] subunit alpha, mitochondrial	340.57	Control
O55100	Synaptogyrin-1	262.69	Control
P80316	T-complex protein 1 subunit epsilon	200.72	Control
P42932	T-complex protein 1 subunit theta	149.24	Control
Q80W22	Threonine synthase-like 2	96.5	Control
Q9Z1T2	Thrombospondin-4	52.59	Control
Q61286	Transcription factor 12	98.9	Control
Q6QR59	TRPM8 channel-associated factor 3	290.23	Control
Q9D906	Ubiquitin-like modifier-activating enzyme ATG7	56.75	Control
P40336	Vacuolar protein sorting-associated protein 26A	139.42	Control
Q62059	Versican core protein	63.41	Control
P29788	Vitronectin	55.89	Control
P46471	26S proteasome regulatory subunit 7	47.83	50 mg/L
P61922	4-aminobutyrate aminotransferase, mitochondrial	391.09	50 mg/L
P10852	4F2 cell-surface antigen heavy chain	152.62	50 mg/L

P61161	Actin-related protein 2	100.9	50 mg/L
Q9WV32	Actin-related protein 2/3 complex subunit 1B	83.28	50 mg/L
Q9CVB6	Actin-related protein 2/3 complex subunit 2	216.14	50 mg/L
Q9JM76	Actin-related protein 2/3 complex subunit 3	574.56	50 mg/L
Q61271	Activin receptor type-1B	44.62	50 mg/L
P31786	Acyl-CoA-binding protein	1758.3	50 mg/L
Q9R0Y5	Adenylate kinase isoenzyme 1	383.65	50 mg/L
P84078	ADP-ribosylation factor 1	78.16	50 mg/L
Q8BSL7	ADP-ribosylation factor 2	54.21	50 mg/L
P61205	ADP-ribosylation factor 3	78.16	50 mg/L
P61750	ADP-ribosylation factor 4	416.87	50 mg/L
P84084	ADP-ribosylation factor 5	416.87	50 mg/L
Q7TPR4	Alpha-actinin-1	59.63	50 mg/L
Q9QYC0	Alpha-adducin	266.87	50 mg/L
Q920R0	Alsin	139.19	50 mg/L
Q7TQF7	Amphiphysin	110.92	50 mg/L
Q7TQI7	Ankyrin repeat and BTB/POZ domain-containing protein 2	93.72	50 mg/L
Q8BZ05	Arf-GAP with Rho-GAP domain, ANK repeat and PH domain-containing protein 2	24.9	50 mg/L
Q497K5	Arrestin domain-containing protein 5	80.25	50 mg/L
Q8R3P0	Aspartoacylase	61.32	50 mg/L
Q9DCX2	ATP synthase subunit d, mitochondrial	768.46	50 mg/L
E9Q4N7	AT-rich interactive domain-containing protein 1B	21.9	50 mg/L
Q61361	Brevican core protein	66.41	50 mg/L
P12367	cAMP-dependent protein kinase type II-alpha regulatory subunit	204.71	50 mg/L
P31324	cAMP-dependent protein kinase type II-beta regulatory subunit	204.71	50 mg/L
B9EHT4	CAP-Gly domain-containing linker protein 3	52.39	50 mg/L
Q65CL1	Catenin alpha-3	41.45	50 mg/L
Q5M8N0	CB1 cannabinoid receptor-interacting protein 1	269.5	50 mg/L
Q91WS0	CDGSH iron-sulfur domain-containing protein 1	189.08	50 mg/L
Q640L3	Cell cycle progression protein 1	60.82	50 mg/L
Q7TSH4	Centriolar coiled-coil protein of 110 kDa	66.84	50 mg/L
Q62036	Centrosomal protein of 131 kDa	44.53	50 mg/L
E9Q309	Centrosome-associated protein 350	26.11	50 mg/L

E9PZM4	Chromodomain-helicase-DNA-binding protein 2	375.14	50 mg/L
Q80YR7	Claspin	89.03	50 mg/L
P63040	Complexin-1	49.54	50 mg/L
P84086	Complexin-2	253.93	50 mg/L
Q9DB77	Cytochrome b-c1 complex subunit 2, mitochondrial	149.5	50 mg/L
P56391	Cytochrome c oxidase subunit 6B1	85.72	50 mg/L
O55071	Cytochrome P450 2B19	63.07	50 mg/L
Q9CX98	Cytochrome P450 2U1	59.31	50 mg/L
O35728	Cytochrome P450 4A14	65.59	50 mg/L
Q99KU1	Dehydrodolichyl diphosphate synthase complex subunit Dhdds	105.52	50 mg/L
Q9EQF6	Dihydropyrimidinase-related protein 5	82.47	50 mg/L
Q80U19	Disheveled-associated activator of morphogenesis 2	38.52	50 mg/L
Q8K4R9	Disks large-associated protein 5	54.05	50 mg/L
Q61881	DNA replication licensing factor MCM7	53.8	50 mg/L
Q8CJ67	Double-stranded RNA-binding protein Staufen homolog 2	90.3	50 mg/L
Q8R0K2	E3 ubiquitin-protein ligase TRIM31	80.78	50 mg/L
Q8BFR5	Elongation factor Tu, mitochondrial	62.53	50 mg/L
P56564	Excitatory amino acid transporter 1	143.9	50 mg/L
Q9ERK4	Exportin-2	79.65	50 mg/L
Q9WVH3	Forkhead box protein O4	75.41	50 mg/L
Q8C0M0	GATOR complex protein WDR59	31.1	50 mg/L
Q9ESZ8	General transcription factor II-I	115.83	50 mg/L
P19157	Glutathione S-transferase P 1	238.47	50 mg/L
P55937	Golgin subfamily A member 3	42.33	50 mg/L
Q91VW5	Golgin subfamily A member 4	65.52	50 mg/L
Q8K349	GTPase IMAP family member 6	69.55	50 mg/L
Q9R0C8	Guanine nucleotide exchange factor VAV3	33.25	50 mg/L
Q61316	Heat shock 70 kDa protein 4	88.69	50 mg/L
Q61699	Heat shock protein 105 kDa	156.6	50 mg/L
P22361	Hepatocyte nuclear factor 1-alpha	72.1	50 mg/L
P61979	Heterogeneous nuclear ribonucleoprotein K	413.21	50 mg/L
Q8R081	Heterogeneous nuclear ribonucleoprotein L	125.22	50 mg/L
Q8VEK3	Heterogeneous nuclear ribonucleoprotein U	63.33	50 mg/L

O88569	Heterogeneous nuclear ribonucleoproteins A2/B1	168.19	50 mg/L
Q91W97	Hexokinase HKDC1	357.2	50 mg/L
O08528	Hexokinase-2	344.36	50 mg/L
Q8R366	Immunoglobulin superfamily member 8	77.23	50 mg/L
Q61739	Integrin alpha-6	56.16	50 mg/L
Q60677	Integrin alpha-E	55.64	50 mg/L
Q8BJD1	Inter-alpha-trypsin inhibitor heavy chain H5	33.53	50 mg/L
Q9QY61	Iroquois-class homeodomain protein IRX-4	116.02	50 mg/L
O54983	Ketimine reductase mu-crystallin	437.71	50 mg/L
P02468	Laminin subunit gamma-1	85.81	50 mg/L
Q8C0R9	Leucine-rich repeat and death domain-containing protein 1	50.31	50 mg/L
A2AWL7	MAX gene-associated protein	22.4	50 mg/L
Q8BJS8	Mdm2-binding protein	33.47	50 mg/L
B1AYB6	Methyl-CpG-binding domain protein 5	130.49	50 mg/L
Q9QYR6	Microtubule-associated protein 1A	26	50 mg/L
P54279	Mismatch repair endonuclease PMS2	81.88	50 mg/L
Q9D6M3	Mitochondrial glutamate carrier 1	935.32	50 mg/L
Q9DB41	Mitochondrial glutamate carrier 2	261.54	50 mg/L
Q63844	Mitogen-activated protein kinase 3	44.51	50 mg/L
Q61885	Myelin-oligodendrocyte glycoprotein	394.33	50 mg/L
Q99MD8	Myoneurin	59.94	50 mg/L
Q9D6J6	NADH dehydrogenase [ubiquinone] flavoprotein 2, mitochondrial	275.26	50 mg/L
Q91VD9	NADH-ubiquinone oxidoreductase 75 kDa subunit, mitochondrial	68.23	50 mg/L
Q91V57	N-chimaerin	127.8	50 mg/L
P06837	Neuromodulin	330.94	50 mg/L
P35802	Neuronal membrane glycoprotein M6-a	62.54	50 mg/L
P97460	Neuronal PAS domain-containing protein 2	157.65	50 mg/L
P97300	Neuroplastin	257.58	50 mg/L
Q61043	Ninein	34.85	50 mg/L
Q8R5A0	N-lysine methyltransferase SMYD2	40.64	50 mg/L
Q02780	Nuclear factor 1 A-type	129.75	50 mg/L
P56716	Oxygen-regulated protein 1	43.45	50 mg/L
P35700	Peroxiredoxin-1	86.99	50 mg/L

O08807	Peroxiredoxin-4	57.42	50 mg/L
Q9D4H9	PHD finger protein 14	68.53	50 mg/L
P53811	Phosphatidylinositol transfer protein beta isoform	83.52	50 mg/L
Q9R0K7	Plasma membrane calcium-transporting ATPase 2	77.91	50 mg/L
P26618	Platelet-derived growth factor receptor alpha	48.55	50 mg/L
P0CG49	Polyubiquitin-B	8981.6	50 mg/L
P0CG50	Polyubiquitin-C	8986.8	50 mg/L
P67778	Prohibitin	112.15	50 mg/L
Q6TDU8	Protein CASC1	29.28	50 mg/L
Q2EMV9	Protein mono-ADP-ribosyltransferase PARP14	33.61	50 mg/L
O55125	Protein NipSnap homolog 1	128.44	50 mg/L
Q3UYC0	Protein phosphatase 1H	136.49	50 mg/L
G3UYX5	Regulator of G-protein signaling 22	61.47	50 mg/L
P70336	Rho-associated protein kinase 2	37.51	50 mg/L
Q9D7H3	RNA 3'-terminal phosphate cyclase	151.46	50 mg/L
A2AGL3	Ryanodine receptor 3	31.45	50 mg/L
Q8C650	Septin-10	112.05	50 mg/L
Q8C1B7	Septin-11	118.18	50 mg/L
Q9DA97	Septin-14	112.05	50 mg/L
Q9R1T4	Septin-6	290.38	50 mg/L
Q91V61	Sideroflexin-3	115.13	50 mg/L
P52019	Squalene monooxygenase	113.26	50 mg/L
Q99JB2	Stomatin-like protein 2, mitochondrial	113.32	50 mg/L
Q9ERG2	Striatin-3	44.66	50 mg/L
Q5SVR0	TBC1 domain family member 9B	32.16	50 mg/L
Q7TN22	Thioredoxin domain-containing protein 16	86.01	50 mg/L
P70399	TP53-binding protein 1	100.25	50 mg/L
P24529	Tyrosine 3-monooxygenase	133.86	50 mg/L
P62983	Ubiquitin-40S ribosomal protein S27a	8981.6	50 mg/L
P62984	Ubiquitin-60S ribosomal protein L40	8981.6	50 mg/L
A2RSJ4	UHRF1-binding protein 1-like	334.57	50 mg/L
Q3U2A8	Valine--tRNA ligase, mitochondrial	33.7	50 mg/L
P62761	Visinin-like protein 1	102.26	50 mg/L

Q60931	Voltage-dependent anion-selective channel protein 3	104.66	50 mg/L
P51863	V-type proton ATPase subunit d 1	140.32	50 mg/L
P50518	V-type proton ATPase subunit E 1	373.39	50 mg/L
Q8BVE3	V-type proton ATPase subunit H	355.93	50 mg/L
Q8K1X1	WD repeat-containing protein 11	52.43	50 mg/L

[a]Uniprot accession ID retrieved from uniport.org database; Negative values of fold change mean down-regulated proteins; 50 mg/L or Control in fold change column means that protein was exclusively found in the respective experimental.

Supplementary table 4. Identified proteins with expression significantly altered in the hippocampus of mice 50 mg/L group vs. 10 mg/L group.

Accession ID[a]	Protein Description	PLGS Score	Fold change
A2AQ07	Tubulin beta-1 chain	168.6	5.99
P02104	Hemoglobin subunit epsilon-Y2	2642.5	5.21
Q61595	Kinectin	92.07	4.9
P02088	Hemoglobin subunit beta-1	2936.3	4.53
P01942	Hemoglobin subunit alpha	1210.9	3.6
P68372	Tubulin beta-4B chain	33674	2.75
Q9D6F9	Tubulin beta-4A chain	16336	2.69
Q8BZQ7	Anaphase-promoting complex subunit 2	87.56	2.66
P99024	Tubulin beta-5 chain	39072	2.64
P61164	Alpha-centractin	397.13	2.59
Q6PHZ2	Calcium/calmodulin-dependent protein kinase type II subunit delta	574.52	2.59
P16858	Glyceraldehyde-3-phosphate dehydrogenase	8044	2.59
Q64524	Histone H2B type 2-E	2291.7	2.53
Q7TMM9	Tubulin beta-2A chain	39321	2.53
Q8R5C5	Beta-centractin	408.8	2.48
Q9CWF2	Tubulin beta-2B chain	39241	2.44
Q9Z1W8	Potassium-transporting ATPase alpha chain 2	299.69	2.41
Q9WV27	Sodium/potassium-transporting ATPase subunit alpha-4	309.34	2.41
Q923T9	Calcium/calmodulin-dependent protein kinase type II subunit gamma	574.52	2.36
P68134	Actin, alpha skeletal muscle	29792	2.27
P62737	Actin, aortic smooth muscle	29766	2.27
P68033	Actin, alpha cardiac muscle 1	29792	2.25
Q9D2U9	Histone H2B type 3-A	2291.7	2.25
P63268	Actin, gamma-enteric smooth muscle	29766	2.23
P10126	Elongation factor 1-alpha 1	326.72	2.03
P60710	Actin, cytoplasmic 1	40198	1.95
Q04447	Creatine kinase B-type	1452.3	1.95
Q922F4	Tubulin beta-6 chain	21599	1.92

P11798	Calcium/calmodulin-dependent protein kinase type II subunit alpha	2519.4	1.82
P53657	Pyruvate kinase PKLR	62.8	1.82
P16330	2',3'-cyclic-nucleotide 3'-phosphodiesterase	417.65	1.79
Q8BFZ3	Beta-actin-like protein 2	7523.9	1.79
P63260	Actin, cytoplasmic 2	40198	1.77
Q61696	Heat shock 70 kDa protein 1A	643.25	1.7
P17879	Heat shock 70 kDa protein 1B	643.25	1.67
P70696	Histone H2B type 1-A	333.92	1.67
P04370	Myelin basic protein	2857	1.63
P60202	Myelin proteolipid protein	4035.3	1.63
P08553	Neurofilament medium polypeptide	146.5	1.63
P18872	Guanine nucleotide-binding protein G(o) subunit alpha	2969.4	1.62
Q03265	ATP synthase subunit alpha, mitochondrial	1417.1	1.6
P0DP28	Calmodulin-3	830.62	1.6
P15105	Glutamine synthetase	424.79	1.6
P0DP27	Calmodulin-2	830.62	1.58
Q62277	Synaptophysin	940.78	1.58
P0DP26	Calmodulin-1	830.62	1.57
P16627	Heat shock 70 kDa protein 1-like	656.84	1.54
Q9D6P8	Calmodulin-like protein 3	1621.7	1.49
Q9ERD7	Tubulin beta-3 chain	32419	1.49
B2RSH2	Guanine nucleotide-binding protein G(i) subunit alpha-1	2040.1	1.48
P63017	Heat shock cognate 71 kDa protein	1105.3	1.48
P17156	Heat shock-related 70 kDa protein 2	754.3	1.48
O88935	Synapsin-1	247.5	1.48
P18760	Cofilin-1	1100.4	1.45
O08553	Dihydropyrimidinase-related protein 2	4617.4	1.43
P08551	Neurofilament light polypeptide	277.72	1.43
P31001	Desmin	57.06	1.42
Q9DC51	Guanine nucleotide-binding protein G(i) subunit alpha	2040.1	1.42
P62983	Ubiquitin-40S ribosomal protein S27a	1318.2	1.4
P20152	Vimentin	103.93	1.4
P46660	Alpha-internexin	299.92	1.39

P08752	Guanine nucleotide-binding protein G(i) subunit alpha-2	2040.1	1.39
P0CG49	Polyubiquitin-B	1318.2	1.39
P0CG50	Polyubiquitin-C	1318.2	1.39
P62984	Ubiquitin-60S ribosomal protein L40	1318.2	1.39
P17742	Peptidyl-prolyl cis-trans isomerase A	1703.2	1.38
P05063	Fructose-bisphosphate aldolase C	810.1	1.36
P63094	Guanine nucleotide-binding protein G(s) subunit alpha isoforms short	2040.1	1.34
P50149	Guanine nucleotide-binding protein G(t) subunit alpha-2	2040.1	1.32
P27600	Guanine nucleotide-binding protein subunit alpha-12	2206	1.32
Q8CGK7	Guanine nucleotide-binding protein G(olf) subunit alpha	2040.1	1.31
Q6R0H7	Guanine nucleotide-binding protein G(s) subunit alpha isoforms XLas	2040.1	1.31
P20612	Guanine nucleotide-binding protein G(t) subunit alpha-1	2040.1	1.31
Q3V3I2	Guanine nucleotide-binding protein G(t) subunit alpha-3	2040.1	1.31
P27601	Guanine nucleotide-binding protein subunit alpha-13	2206	1.31
P05064	Fructose-bisphosphate aldolase A	2667	1.26
P60879	Synaptosomal-associated protein 25	253.29	1.23
P07724	Serum albumin	249.47	1.22
P05213	Tubulin alpha-1B chain	14800	1.16
P68369	Tubulin alpha-1A chain	14742	1.15
P05214	Tubulin alpha-3 chain	8020.7	1.15
P68373	Tubulin alpha-1C chain	13174	1.11
P68368	Tubulin alpha-4A chain	12233	1.11
P05202	Aspartate aminotransferase, mitochondrial	211.16	1.08
Q68FD5	Clathrin heavy chain 1	192.64	1.08
P17183	Gamma-enolase	2014.2	1.07
A2AL36	Centriolin	70.22	-0.28
Q64467	Glyceraldehyde-3-phosphate dehydrogenase, testis-specific	534.1	-0.41
Q9CQN1	Heat shock protein 75 kDa, mitochondrial	1035.3	-0.5
P20801	Troponin C, skeletal muscle	557.51	-0.52
P50518	V-type proton ATPase subunit E 1	302.13	-0.53
Q91VD9	NADH-ubiquinone oxidoreductase 75 kDa subunit, mitochondrial	303.78	-0.56
P06837	Neuromodulin	347.57	-0.58
Q9Z2Q6	Septin-5	356.87	-0.58

O08749	Dihydrolipoyl dehydrogenase, mitochondrial	83.56	-0.59
Q61011	Guanine nucleotide-binding protein G(I)/G(S)/G(T) subunit beta-3	1057.6	-0.59
Q8CGP6	Histone H2A type 1-H	566.36	-0.59
C0HKE1	Histone H2A type 1-B	566.36	-0.61
C0HKE4	Histone H2A type 1-E	566.36	-0.61
Q6GSS7	Histone H2A type 2-A	566.36	-0.61
Q64523	Histone H2A type 2-C	566.36	-0.61
Q8R1M2	Histone H2A.J	566.36	-0.61
P62806	Histone H4	3283.9	-0.61
P29387	Guanine nucleotide-binding protein subunit beta-4	3728.7	-0.62
C0HKE3	Histone H2A type 1-D	566.36	-0.62
Q8CGP5	Histone H2A type 1-F	566.36	-0.62
C0HKE5	Histone H2A type 1-G	566.36	-0.62
C0HKE7	Histone H2A type 1-N	566.36	-0.62
C0HKE8	Histone H2A type 1-O	566.36	-0.62
C0HKE9	Histone H2A type 1-P	566.36	-0.62
Q8BFU2	Histone H2A type 3	566.36	-0.62
P63101	14-3-3 protein zeta/delta	4355.7	-0.63
Q9CR68	Cytochrome b-c1 complex subunit Rieske, mitochondrial	862.55	-0.63
C0HKE2	Histone H2A type 1-C	566.36	-0.63
C0HKE6	Histone H2A type 1-I	566.36	-0.63
Q8CGP7	Histone H2A type 1-K	566.36	-0.63
Q8BMF4	Dihydrolipoyllysine-residue acetyltransferase component of pyruvate dehydrogenase complex, mitochondrial	157.68	-0.64
P08228	Superoxide dismutase [Cu-Zn]	561.16	-0.65
P62259	14-3-3 protein epsilon	3377.9	-0.66
P68254	14-3-3 protein theta	3427.4	-0.66
Q91XV3	Brain acid soluble protein 1	334.05	-0.66
P20029	Endoplasmic reticulum chaperone BiP	1685.2	-0.66
P16125	L-lactate dehydrogenase B chain	1913.3	-0.66
Q9QYR6	Microtubule-associated protein 1A	42.54	-0.66
Q9CQV8	14-3-3 protein beta/alpha	3457.3	-0.67
P61982	14-3-3 protein gamma	4013.2	-0.67

P62880	Guanine nucleotide-binding protein G(I)/G(S)/G(T) subunit beta-2	4153.3	-0.67
P28663	Beta-soluble NSF attachment protein	448.22	-0.68
P19783	Cytochrome c oxidase subunit 4 isoform 1, mitochondrial	1353.2	-0.68
Q62420	Endophilin-A1	534.27	-0.68
P07901	Heat shock protein HSP 90-alpha	1228	-0.68
Q3UX10	Tubulin alpha chain-like 3	235.27	-0.68
Q8BVE3	V-type proton ATPase subunit H	172.23	-0.68
Q64433	10 kDa heat shock protein, mitochondrial	733.54	-0.69
O70456	14-3-3 protein sigma	3382.1	-0.69
P51881	ADP/ATP translocase 2	492.15	-0.69
Q3V132	ADP/ATP translocase 4	274.71	-0.69
Q01768	Nucleoside diphosphate kinase B	750.12	-0.69
Q91ZZ3	Beta-synuclein	3392	-0.7
P62874	Guanine nucleotide-binding protein G(I)/G(S)/G(T) subunit beta-1	4165.7	-0.7
P00342	L-lactate dehydrogenase C chain	1010.2	-0.7
P46097	Synaptotagmin-2	124.21	-0.7
P68510	14-3-3 protein eta	3427.4	-0.71
Q8BSL7	ADP-ribosylation factor 2	1134.6	-0.71
Q9DB77	Cytochrome b-c1 complex subunit 2, mitochondrial	430.39	-0.71
P08249	Malate dehydrogenase, mitochondrial	1459.2	-0.71
Q9D051	Pyruvate dehydrogenase E1 component subunit beta, mitochondrial	145.38	-0.71
P14094	Sodium/potassium-transporting ATPase subunit beta-1	3370.7	-0.71
Q64475	Histone H2B type 1-B	2822.6	-0.72
P10853	Histone H2B type 1-F/J/L	2822.6	-0.72
Q64525	Histone H2B type 2-B	2822.6	-0.72
Q9DD03	Ras-related protein Rab-13	308.37	-0.72
Q9R0N5	Synaptotagmin-5	93.86	-0.72
Q6ZWY9	Histone H2B type 1-C/E/G	2822.6	-0.73
Q64478	Histone H2B type 1-H	2822.6	-0.73
Q8CGP1	Histone H2B type 1-K	2822.6	-0.73
P10854	Histone H2B type 1-M	2822.6	-0.73
Q8CGP2	Histone H2B type 1-P	2822.6	-0.73
Q8CGP0	Histone H2B type 3-B	2291.7	-0.73

P35802	Neuronal membrane glycoprotein M6-a	67.63	-0.73
P70296	Phosphatidylethanolamine-binding protein 1	2276.6	-0.73
Q64436	Potassium-transporting ATPase alpha chain 1	20.73	-0.73
Q64332	Synapsin-2	143.9	-0.73
P06151	L-lactate dehydrogenase A chain	1477.7	-0.74
P01831	Thy-1 membrane glycoprotein	388.2	-0.74
P84078	ADP-ribosylation factor 1	1615.3	-0.75
P61205	ADP-ribosylation factor 3	1615.3	-0.75
P48962	ADP/ATP translocase 1	640.34	-0.76
P20357	Microtubule-associated protein 2	398.89	-0.76
P46096	Synaptotagmin-1	467.04	-0.76
P31786	Acyl-CoA-binding protein	1471.6	-0.77
P47857	ATP-dependent 6-phosphofructokinase, muscle type	386.14	-0.78
P02089	Hemoglobin subunit beta-2	2642.5	-0.78
Q9DBJ1	Phosphoglycerate mutase 1	1170.7	-0.78
O55042	Alpha-synuclein	1500.1	-0.79
P56480	ATP synthase subunit beta, mitochondrial	2086.2	-0.79
P00405	Cytochrome c oxidase subunit 2	282.96	-0.79
P12787	Cytochrome c oxidase subunit 5A, mitochondrial	2092.4	-0.79
P26443	Glutamate dehydrogenase 1, mitochondrial	120.26	-0.79
S4R2M7	Phosphoglycerate kinase	90.57	-0.79
Q61598	Rab GDP dissociation inhibitor beta	879.55	-0.79
Q62261	Spectrin beta chain, non-erythrocytic 1	218.26	-0.79
O08599	Syntaxin-binding protein 1	1513	-0.79
P17710	Hexokinase-1	96.46	-0.8
P17751	Triosephosphate isomerase	696.18	-0.8
Q60930	Voltage-dependent anion-selective channel protein 2	741.88	-0.8
P10649	Glutathione S-transferase Mu 1	1091.2	-0.81
Q02053	Ubiquitin-like modifier-activating enzyme 1	102.99	-0.81
Q8BZ98	Dynamin-3	288.11	-0.82
P15532	Nucleoside diphosphate kinase A	999.05	-0.82
P09041	Phosphoglycerate kinase 2	101.21	-0.82
Q9D6R2	Isocitrate dehydrogenase [NAD] subunit alpha, mitochondrial	98.41	-0.83

Q8VEM8	Phosphate carrier protein, mitochondrial	425.26	-0.83
P55258	Ras-related protein Rab-8A	1045.2	-0.83
P39054	Dynamin-2	296.96	-0.84
P62631	Elongation factor 1-alpha 2	51.32	-0.84
P43006	Excitatory amino acid transporter 2	1126	-0.84
P06745	Glucose-6-phosphate isomerase	593.01	-0.84
Q61171	Peroxiredoxin-2	1065.8	-0.84
P63011	Ras-related protein Rab-3A	2770.6	-0.84
Q9CZT8	Ras-related protein Rab-3B	2222.7	-0.84
P62823	Ras-related protein Rab-3C	2222.7	-0.84
P35276	Ras-related protein Rab-3D	2349	-0.84
P61028	Ras-related protein Rab-8B	1045.2	-0.84
P48453	Serine/threonine-protein phosphatase 2B catalytic subunit beta isoform	206.19	-0.84
Q8VDN2	Sodium/potassium-transporting ATPase subunit alpha-1	299.61	-0.84
Q6PIE5	Sodium/potassium-transporting ATPase subunit alpha-2	391.86	-0.84
Q60932	Voltage-dependent anion-selective channel protein 1	1285.5	-0.84
Q9DB20	ATP synthase subunit O, mitochondrial	3233.6	-0.85
P14152	Malate dehydrogenase, cytoplasmic	1010.9	-0.85
P50396	Rab GDP dissociation inhibitor alpha	1806.3	-0.85
P63328	Serine/threonine-protein phosphatase 2B catalytic subunit alpha isoform	464.27	-0.85
Q8K386	Ras-related protein Rab-15	905.96	-0.86
P62821	Ras-related protein Rab-1A	928.3	-0.86
P28652	Calcium/calmodulin-dependent protein kinase type II subunit beta	608.48	-0.87
P09411	Phosphoglycerate kinase 1	90.57	-0.87
Q6PIC6	Sodium/potassium-transporting ATPase subunit alpha-3	461.07	-0.87
P50516	V-type proton ATPase catalytic subunit A	269.63	-0.87
P17182	Alpha-enolase	2930.6	-0.88
Q62188	Dihydropyrimidinase-related protein 3	174.48	-0.88
Q76MZ3	Serine/threonine-protein phosphatase 2A 65 kDa regulatory subunit A alpha isoform	143.18	-0.88
P97427	Dihydropyrimidinase-related protein 1	818.92	-0.9
P52480	Pyruvate kinase PKM	3457.2	-0.9
P39053	Dynamin-1	1744.9	-0.91

Q9Z1B3	1-phosphatidylinositol 4,5-bisphosphate phosphodiesterase beta-1	41.48	10 mg/L
Q60597	2-oxoglutarate dehydrogenase, mitochondrial	92.99	10 mg/L
Q5SSL4	Active breakpoint cluster region-related protein	51.4	10 mg/L
Q80Y20	Alkylated DNA repair protein alkB homolog 8	129.16	10 mg/L
Q8C6Y6	Ankyrin repeat and SOCS box protein 14	57.7	10 mg/L
O35643	AP-1 complex subunit beta-1	60.21	10 mg/L
Q9DBG3	AP-2 complex subunit beta	110.45	10 mg/L
P06728	Apolipoprotein A-IV	180.65	10 mg/L
Q99KN1	Arrestin domain-containing protein 1	175.26	10 mg/L
Q91VR2	ATP synthase subunit gamma, mitochondrial	185.97	10 mg/L
P97450	ATP synthase-coupling factor 6, mitochondrial	785.56	10 mg/L
Q9DC29	ATP-binding cassette sub-family B member 6, mitochondrial	32.46	10 mg/L
Q99PU8	ATP-dependent RNA helicase DHX30	149.18	10 mg/L
Q9Z2H5	Band 4.1-like protein 1	55.35	10 mg/L
Q9QYB8	Beta-adducin	84.36	10 mg/L
Q8BKX1	Brain-specific angiogenesis inhibitor 1-associated protein 2	130.66	10 mg/L
P35762	CD81 antigen	627.76	10 mg/L
Q99N28	Cell adhesion molecule 3	230.14	10 mg/L
A2A6Q5	Cell division cycle protein 27 homolog	59.73	10 mg/L
Q6A065	Centrosomal protein of 170 kDa	88.12	10 mg/L
A2A8L1	Chromodomain-helicase-DNA-binding protein 5	40.82	10 mg/L
Q9EPU4	Cleavage and polyadenylation specificity factor subunit 1	137.64	10 mg/L
Q8CDI7	Coiled-coil domain-containing protein 150	73.6	10 mg/L
Q8CI04	Conserved oligomeric Golgi complex subunit 3	29.61	10 mg/L
P19536	Cytochrome c oxidase subunit 5B, mitochondrial	392.36	10 mg/L
P48771	Cytochrome c oxidase subunit 7A2, mitochondrial	514.4	10 mg/L
Q8C4S8	DENN domain-containing protein 2A	64.83	10 mg/L
Q811D0	Disks large homolog 1	78.4	10 mg/L
Q91XM9	Disks large homolog 2	98.04	10 mg/L
Q62108	Disks large homolog 4	206.56	10 mg/L
Q6PFD5	Disks large-associated protein 3	52.24	10 mg/L

Q4U2R1	E3 ubiquitin-protein ligase HERC2	88.09	10 mg/L
Q9DCS3	Enoyl-[acyl-carrier-protein] reductase, mitochondrial	119.84	10 mg/L
Q0VAV2	Exophilin-5	38.17	10 mg/L
P47754	F-actin-capping protein subunit alpha-2	227.89	10 mg/L
Q80X90	Filamin-B	32.25	10 mg/L
D3Z7P3	Glutaminase kidney isoform, mitochondrial	99.06	10 mg/L
P46425	Glutathione S-transferase P 2	495.07	10 mg/L
Q9WV07	Hydroperoxide isomerase ALOXE3	59.28	10 mg/L
Q3KNY0	Immunoglobulin-like and fibronectin type III domain-containing protein 1	29.85	10 mg/L
Q571I4	Inactive tyrosine-protein kinase PRAG1	58.94	10 mg/L
Q80V86	Integrator complex subunit 8	71.24	10 mg/L
A6X935	Inter alpha-trypsin inhibitor, heavy chain 4	42.89	10 mg/L
Q60625	Intercellular adhesion molecule 5	48.95	10 mg/L
Q9QZ85	Interferon-inducible GTPase 1	58.34	10 mg/L
Q62406	Interleukin-1 receptor-associated kinase 1	142.9	10 mg/L
A2CG49	Kalirin	82.96	10 mg/L
P11369	LINE-1 retrotransposable element ORF2 protein	40.09	10 mg/L
Q9JI18	Low-density lipoprotein receptor-related protein 1B	39.31	10 mg/L
Q9JJ78	Lymphokine-activated killer T-cell-originated protein kinase	69.55	10 mg/L
O08539	Myc box-dependent-interacting protein 1	320.05	10 mg/L
Q9DCT2	NADH dehydrogenase [ubiquinone] iron-sulfur protein 3, mitochondrial	107.77	10 mg/L
P52503	NADH dehydrogenase [ubiquinone] iron-sulfur protein 6, mitochondrial	194.46	10 mg/L
Q6GQX2	Nck-associated protein 5-like	147.69	10 mg/L
Q8R007	Nectin-4	72.22	10 mg/L
P70211	Netrin receptor DCC	45.19	10 mg/L
Q9QXX8	Nuclear fragile X mental retardation-interacting protein 1	98.96	10 mg/L
Q61937	Nucleophosmin	82.67	10 mg/L
O54998	Peptidyl-prolyl cis-trans isomerase FKBP7	99.86	10 mg/L
Q5BL07	Peroxisome biogenesis factor 1	140.96	10 mg/L
Q91YL7	PGAP2-interacting protein	52.95	10 mg/L
O70167	Phosphatidylinositol 4-phosphate 3-kinase C2 domain-containing subunit gamma	66.06	10 mg/L

O70250	Phosphoglycerate mutase 2	112.61	10 mg/L
Q8CDG1	Piwi-like protein 2	131.71	10 mg/L
O35129	Prohibitin-2	402.09	10 mg/L
Q9QXV0	ProSAAS	113.13	10 mg/L
Q61207	Prosaposin	74.57	10 mg/L
Q8BHZ0	Protein FAM49A	149.49	10 mg/L
Q9CU24	Protein THEMIS3	47.42	10 mg/L
Q8K183	Pyridoxal kinase	111.98	10 mg/L
P35294	Ras-related protein Rab-19	293.2	10 mg/L
P24549	Retinal dehydrogenase 1	132.8	10 mg/L
Q8BRH3	Rho GTPase-activating protein 19	82.39	10 mg/L
Q8BWA8	Rho guanine nucleotide exchange factor 19	263.26	10 mg/L
Q9CZC8	Secernin-1	250.9	10 mg/L
B2RXR6	Serine/threonine-protein phosphatase 6 regulatory ankyrin repeat subunit B	116.3	10 mg/L
Q4VA53	Sister chromatid cohesion protein PDS5 homolog B	44.45	10 mg/L
Q3UHA3	Spatacsin	34.61	10 mg/L
Q8BWF0	Succinate-semialdehyde dehydrogenase, mitochondrial	188.93	10 mg/L
P61264	Syntaxin-1B	374.9	10 mg/L
A6H6E9	Tetratricopeptide repeat protein 23-like	78.77	10 mg/L
Q3UR70	Transforming growth factor-beta receptor-associated protein 1	101.94	10 mg/L
Q00993	Tyrosine-protein kinase receptor UFO	51.64	10 mg/L
P56399	Ubiquitin carboxyl-terminal hydrolase 5	68.64	10 mg/L
Q9DBP5	UMP-CMP kinase	91.98	10 mg/L
Q62059	Versican core protein	90.05	10 mg/L
P63024	Vesicle-associated membrane protein 3	40.24	10 mg/L
P61161	Actin-related protein 2	100.9	50 mg/L
Q9R0Q6	Actin-related protein 2/3 complex subunit 1A	103.13	50 mg/L
Q9WV32	Actin-related protein 2/3 complex subunit 1B	83.28	50 mg/L
Q9CVB6	Actin-related protein 2/3 complex subunit 2	216.14	50 mg/L
Q9JM76	Actin-related protein 2/3 complex subunit 3	574.56	50 mg/L
Q99JY9	Actin-related protein 3	1211.34	50 mg/L

Q61271	Activin receptor type-1B	44.62	50 mg/L
Q9R0Y5	Adenylate kinase isoenzyme 1	383.65	50 mg/L
P40124	Adenylyl cyclase-associated protein 1	467.05	50 mg/L
Q920R0	Alsin	139.19	50 mg/L
Q7TQI7	Ankyrin repeat and BTB/POZ domain-containing protein 2	93.72	50 mg/L
P84091	AP-2 complex subunit mu	254.17	50 mg/L
Q8BZ05	Arf-GAP with Rho-GAP domain, ANK repeat and PH domain-containing protein 2	24.9	50 mg/L
Q497K5	Arrestin domain-containing protein 5	80.25	50 mg/L
Q8R3P0	Aspartoacylase	61.32	50 mg/L
E9Q4N7	AT-rich interactive domain-containing protein 1B	21.9	50 mg/L
P12367	cAMP-dependent protein kinase type II-alpha regulatory subunit	204.71	50 mg/L
P31324	cAMP-dependent protein kinase type II-beta regulatory subunit	204.71	50 mg/L
B9EHT4	CAP-Gly domain-containing linker protein 3	52.39	50 mg/L
Q5M8N0	CB1 cannabinoid receptor-interacting protein 1	269.5	50 mg/L
Q91WS0	CDGSH iron-sulfur domain-containing protein 1	189.08	50 mg/L
Q640L3	Cell cycle progression protein 1	60.82	50 mg/L
Q7TSH4	Centriolar coiled-coil protein of 110 kDa	66.84	50 mg/L
Q62036	Centrosomal protein of 131 kDa	44.53	50 mg/L
E9Q309	Centrosome-associated protein 350	26.11	50 mg/L
E9PZM4	Chromodomain-helicase-DNA-binding protein 2	375.14	50 mg/L
Q80YR7	Claspin	89.03	50 mg/L
Q62425	Cytochrome c oxidase subunit NDUFA4	1748.56	50 mg/L
O55071	Cytochrome P450 2B19	63.07	50 mg/L
Q9CX98	Cytochrome P450 2U1	59.31	50 mg/L
O35728	Cytochrome P450 4A14	65.59	50 mg/L
Q99KU1	Dehydrodolichyl diphosphate synthase complex subunit Dhdds	105.52	50 mg/L
Q80U19	Disheveled-associated activator of morphogenesis 2	38.52	50 mg/L
Q8K4R9	Disks large-associated protein 5	54.05	50 mg/L
Q61881	DNA replication licensing factor MCM7	53.8	50 mg/L
Q8CJ67	Double-stranded RNA-binding protein Staufen homolog 2	90.3	50 mg/L
Q8R0K2	E3 ubiquitin-protein ligase TRIM31	80.78	50 mg/L

P56564	Excitatory amino acid transporter 1	143.9	50 mg/L
Q9WVH3	Forkhead box protein O4	75.41	50 mg/L
Q8C0M0	GATOR complex protein WDR59	31.1	50 mg/L
Q9ESZ8	General transcription factor II-I	115.83	50 mg/L
Q8CI94	Glycogen phosphorylase, brain form	37.32	50 mg/L
Q9ET01	Glycogen phosphorylase, liver form	25.65	50 mg/L
Q9WUB3	Glycogen phosphorylase, muscle form	25.65	50 mg/L
Q9CW79	Golgin subfamily A member 1	86.47	50 mg/L
P55937	Golgin subfamily A member 3	42.33	50 mg/L
Q91VW5	Golgin subfamily A member 4	65.52	50 mg/L
Q8K349	GTPase IMAP family member 6	69.55	50 mg/L
Q9R0C8	Guanine nucleotide exchange factor VAV3	33.25	50 mg/L
P22361	Hepatocyte nuclear factor 1-alpha	72.1	50 mg/L
P61979	Heterogeneous nuclear ribonucleoprotein K	413.21	50 mg/L
Q8R081	Heterogeneous nuclear ribonucleoprotein L	125.22	50 mg/L
Q8VEK3	Heterogeneous nuclear ribonucleoprotein U	63.33	50 mg/L
O88569	Heterogeneous nuclear ribonucleoproteins A2/B1	168.19	50 mg/L
Q91W97	Hexokinase HKDC1	357.2	50 mg/L
O08528	Hexokinase-2	344.36	50 mg/L
P70349	Histidine triad nucleotide-binding protein 1	328.07	50 mg/L
Q8R366	Immunoglobulin superfamily member 8	77.23	50 mg/L
Q61739	Integrin alpha-6	56.16	50 mg/L
Q60677	Integrin alpha-E	55.64	50 mg/L
Q8BJD1	Inter-alpha-trypsin inhibitor heavy chain H5	33.53	50 mg/L
Q9QY61	Iroquois-class homeodomain protein IRX-4	116.02	50 mg/L
Q9QXL2	Kinesin-like protein KIF21A	71.51	50 mg/L
Q8C0R9	Leucine-rich repeat and death domain-containing protein 1	50.31	50 mg/L
A2AWL7	MAX gene-associated protein	22.4	50 mg/L
Q8BJS8	Mdm2-binding protein	33.47	50 mg/L
B1AYB6	Methyl-CpG-binding domain protein 5	130.49	50 mg/L
Q8K1A0	Methyltransferase-like protein 5	88.52	50 mg/L

P54279	Mismatch repair endonuclease PMS2	81.88	50 mg/L
Q99MD8	Myoneurin	59.94	50 mg/L
Q99LC3	NADH dehydrogenase [ubiquinone] 1 alpha subcomplex subunit 10, mitochondrial	298.33	50 mg/L
Q91V57	N-chimaerin	127.8	50 mg/L
Q810U3	Neurofascin	61.91	50 mg/L
P97460	Neuronal PAS domain-containing protein 2	157.65	50 mg/L
Q61043	Ninein	34.85	50 mg/L
Q8R5A0	N-lysine methyltransferase SMYD2	40.64	50 mg/L
Q02780	Nuclear factor 1 A-type	129.75	50 mg/L
P56716	Oxygen-regulated protein 1	43.45	50 mg/L
Q9D4H9	PHD finger protein 14	68.53	50 mg/L
P53811	Phosphatidylinositol transfer protein beta isoform	83.52	50 mg/L
G5E829	Plasma membrane calcium-transporting ATPase 1	93.23	50 mg/L
Q9R0K7	Plasma membrane calcium-transporting ATPase 2	77.91	50 mg/L
P26618	Platelet-derived growth factor receptor alpha	48.55	50 mg/L
Q6TDU8	Protein CASC1	29.28	50 mg/L
Q2EMV9	Protein mono-ADP-ribosyltransferase PARP14	33.61	50 mg/L
Q3UYC0	Protein phosphatase 1H	136.49	50 mg/L
E5FYH1	Protein TOPAZ1	46.16	50 mg/L
P35486	Pyruvate dehydrogenase E1 component subunit alpha, somatic form, mitochondrial	75.99	50 mg/L
G3UYX5	Regulator of G-protein signaling 22	61.47	50 mg/L
Q9ES97	Reticulon-3	88.22	50 mg/L
P70336	Rho-associated protein kinase 2	37.51	50 mg/L
Q9D7H3	RNA 3'-terminal phosphate cyclase	151.46	50 mg/L
A2AGL3	Ryanodine receptor 3	31.45	50 mg/L
Q91V61	Sideroflexin-3	115.13	50 mg/L
Q923Q2	StAR-related lipid transfer protein 13	72.57	50 mg/L
Q99JB2	Stomatin-like protein 2, mitochondrial	113.32	50 mg/L
Q9ERG2	Striatin-3	44.66	50 mg/L
Q9Z2I9	Succinate--CoA ligase [ADP-forming] subunit beta, mitochondrial	44.71	50 mg/L
Q8CHC4	Synaptojanin-1	51.04	50 mg/L

Q5SVR0	TBC1 domain family member 9B	32.16	50 mg/L
Q7TN22	Thioredoxin domain-containing protein 16	86.01	50 mg/L
P70399	TP53-binding protein 1	100.25	50 mg/L
P42669	Transcriptional activator protein Pur-alpha	216.84	50 mg/L
Q9R1Q8	Transgelin-3	312.49	50 mg/L
P24529	Tyrosine 3-monooxygenase	133.86	50 mg/L
Q7TQI3	Ubiquitin thioesterase OTUB1	613.88	50 mg/L
A2RSJ4	UHRF1-binding protein 1-like	334.57	50 mg/L
Q3U2A8	Valine--tRNA ligase, mitochondrial	33.7	50 mg/L
Q8K1X1	WD repeat-containing protein 11	52.43	50 mg/L

[a]Uniprot accession ID retrieved from uniport.org database; Negative values of fold change mean down-regulated proteins; 10 mg/L or 50 mg/L in fold change column means that protein was exclusively found in the respective experimental.

REFERÊNCIAS

AGNELLI, P.B. **Variação do índice CPOD do Brasil no período de 1980 a 2010**. Rev. bras. odontol., Rio de Janeiro, v. 72, n. 1/2, p. 10-5, 2015.

ALVARINHO, S. B. E MARTINELLI, J. R. **Utilização de alumina para a remoção de fluoretos em águas e efluentes.** Cerâmica [online]. 2000, v. 46, n. 298 [Acessado 4 Novembro 2021], pp. 104-117.

AOUN, A., DARWICHE, F., AL HAYEK, S., & DOUMIT, J**. The Fluoride Debate: The Pros and Cons of Fluoridation**. *Preventive nutrition and food science*, *23*(3), 171–180, 2018.

BANALA, R.R. e KARNATI, P.R. **Vitamin A Deficiency: An Oxidative Stress Marker In Sodium Fluoride (Naf) Induced Oxidative Damage In Developing Rat Brain**. *Int J Dev Neurosci*. 47(Pt B):298–303, 2015.

BARTOS, M., GUMILAR, F., GALLEGOS, C. E., BRAS, C., DOMINGUEZ, S., MÓNACO, N., ESANDI, M., BOUZAT, C., CANCELA, L. M., & MINETTI, A. **Alterations in the memory of rat offspring exposed to low levels of fluoride during gestation and lactation: Involvement of the α7 nicotinic receptor and oxidative stress.** *Reprod Toxicol*. 2018;81:108-114.

BUZALAF MAR & LEVY SM. **Fluoride intake of children: considerations for dental caries and dental fluorosis.** *Monogr Oral Sci*.; 22:1–19, 2011.

CAO SR, LI YF. **The evaluation of indoor air quality in areas of endemic fluorosis caused by coal combustion.** In: *Proceedings of the XIX Conference of the International Society for Fluoride Research*, Kyoto, Japan. Kyoto, Department of Hygiene and Public Health, Osaka Medical College, p. 38, 1992.

CAO, Q., WANG, J., HAO, Y., ZHAO, F., FU, R., YU, Y., WANG, J., NIU, R., BIAN, S., & SUN, Z. **Exercise Ameliorates Fluoride-induced Anxiety- and Depression-like Behavior in Mice: Role of GABA** [publicado online, *ahead of print*, 2021 Apr 6]. *Biol Trace Elem Res*.

CHOI, A.L.; SUN, G.; ZHANG, Y.; GRANDJEAN, P. Developmental fluoride neurotoxicity: a systematic review and meta-analysis. Environmental health perspectives, 120, 1362-1368, 2012.

CORTES DF, ELLWOOD RP, MULLANE DMO, BASTOS JRM. **Drinking water fluoride levels, dental fluorosis and caries experience in Brazil**. *J Public Health Dent* 1996; 56(4):226-228.

DEC, K., ŁUKOMSKA, A., SKONIECZNA-ŻYDECKA, K., KOLASA-WOŁOSIUK, A., TARNOWSKI, M., BARANOWSKA-BOSIACKA, I., & GUTOWSKA, I. **Long-term exposure to fluoride as a factor promoting changes in the expression and activity of cyclooxygenases (COX1 and COX2) in various rat brain structures.** *Neurotoxicology*. 2019;74:81-90.

DIONIZIO, A., MELO, C., SABINO-ARIAS, I. T., ARAUJO, T. T., VENTURA, T., LEITE, A. L., SOUZA, S., SANTOS, E. X., HEUBEL, A. D., SOUZA, J. G., PERLES, J., ZANONI, J. N., & BUZALAF, M. **Effects of acute fluoride exposure on the jejunum**

and ileum of rats: Insights from proteomic and enteric innervation analysis. *Sci Total Environ*. 2020;741:140419, 2020.

DUAN Q, JIAO J, CHEN X, WANG X. **Association between water fluoride and the level of children's intelligence: a dose response meta-analysis**, *Public Health, 54, 87-97,* 2018.

FENG Z, LIANG C, MANTHARI RK, WANG C, ZHANG J. **Effects of Fluoride on Autophagy in Mouse Sertoli Cells**. *Biol Trace Elem Res*. 2019;187(2):499-505.

FERREIRA, M., ARAGÃO, W., BITTENCOURT, L. O., PUTY, B., DIONIZIO, A., SOUZA, M., BUZALAF, M., DE OLIVEIRA, E. H., CRESPO-LOPEZ, M. E., & LIMA, R. R. **Fluoride exposure during pregnancy and lactation triggers oxidative stress and molecular changes in hippocampus of offspring rats.** *Ecotoxicology and environmental safety*, *208*, 111437, 2021.

GE, Y., CHEN, L., YIN, Z., SONG, X., RUAN, T., HUA, L., LIU, J., WANG, J., & NING, H. **Fluoride-induced alterations of synapse-related proteins in the cerebral cortex of ICR offspring mouse brain.** *Chemosphere*. 2018;201:874-883.

JIANG Y, GUO X, SUN Q, SHAN Z, TENG W. **Effects of Excess Fluoride and Iodide on Thyroid Function and Morphology.** *Biol Trace Elem Res*. 2016;170(2):382-389.

KIM, Y., KIM, JY. & KIM, K. Geochemical characteristics of fluoride in groundwater of Gimcheon, Korea: lithogenic and agricultural origins. Environ Earth Sci 63, 1139–1148 (2011).

LIMA, L., MIRANDA, G., ARAGÃO, W., BITTENCOURT, L. O., DOS SANTOS, S. M., DE SOUZA, M., NOGUEIRA, L. S., DE OLIVEIRA, E., MONTEIRO, M. C., DIONIZIO, A., LEITE, A. L., PESSAN, J. P., BUZALAF, M., & LIMA, R. R. **Effects of Fluoride on Submandibular Glands of Mice: Changes in Oxidative Biochemistry, Proteomic Profile, and Genotoxicity.** *Frontiers in pharmacology*, *12*, 715394, 2021.

LOPES, G.O.; MARTINS FERREIRA, M.K.; DAVIS, L.; BITTENCOURT, L.O.; BRAGANÇA ARAGÃO, W.A.; DIONIZIO, A.; RABELO BUZALAF, M.A.; CRESPO-LOPEZ, M.E.; MAIA, C.S.F.; LIMA, R.R. **Effects of Fluoride Long-Term Exposure over the Cerebellum: Global Proteomic Profile**, Oxidative Biochemistry, Cell Density, and Motor Behavior Evaluation. International journal of molecular sciences 2020, 21,.

MIRANDA, G.H.N.; ALVARENGA, M.O.P.; FERREIRA, M.K.M.; PUTY, B.; BITTENCOURT, L.O.; FAGUNDES, N.C.F.; PESSAN, J.P.; BUZALAF, M.A.R.; LIMA, R.R. **A systematic review and meta-analysis of the association between fluoride exposure and neurological disorders**. Scientific Reports 2021. *In press.*

MOIMAZ SA, SALIBA NA, SALIBA O, SUMIDA DH, SOUZA NP, CHIBA FY, GARBIN CA. **Water fluoridation in 40 Brazilian cities: 7 year analysis.** *J Appl Oral Sci*. Jan-Feb;21(1):13-9, 2013.

MUKHERJEE, I., SINGH, U.K. **Groundwater fluoride contamination, probable release, and containment mechanisms: a review on Indian context.** Environ Geochem Health 40, 2259–2301, 2018.

NARVAI PC. Cárie dentária e flúor: uma relação do século XX. ***Ciência & Saúde Coletiva***, 5(2):381-392, 2000.

NCBI. NATIONAL CENTER FOR BIOTECHNOLOGY INFORMATION. PubChem Compound Summary for CID 28179, **Fluoride ion.** Disponível em: https://pubchem.ncbi.nlm.nih.gov/compound/Fluoride-ion. Acesso em: 5 de novembro de 2021.

NIU, R., CHEN, H., MANTHARI, R. K., SUN, Z., WANG, J., ZHANG, J., & WANG, J. **Effects of fluoride on synapse morphology and myelin damage in mouse hippocampus.** *Chemosphere*. 2018;194:628-633.

OMS. ORGANIZAÇÃO MUNDIAL DA SAÚDE. **Fluorides**. Environmental Health Criteria 227. Genebra: World Health Organization. 2002.

PECKHAM, S., & AWOFESO, N. **Water fluoridation: a critical review of the physiological effects of ingested fluoride as a public health intervention.** TheScientificWorldJournal, 293019, 2014.

PUTY, B.; BITTENCOURT, L.O.; NOGUEIRA, I.C.; BUZALAF, M.A.R.; OLIVEIRA, E.H.; LIMA, R.R. **Human cultured IMR-32 neuronal-like and U87 glial-like cells have different patterns of toxicity under fluoride exposure.** PloS one, 16, e0251200, 2021.

RAMIRES, I; BUZALAF, MAR. **A fluoretação da água de abastecimento público e seus benefícios no controle da cárie dentária: cinqüenta anos no Brasil.** Ciência & Saúde Coletiva, v. 12, p. 1057-1065, 2007.

REDDY, Y.P.; TIWARI, S.K.; SHAIK, A.P.; ALSAEED, A.; SULTANA, A. e REDDY, P.K. **Effect Of Sodium Fluoride On Neuroimmunological Parameters, Oxidative Stress And Antioxidative Defenses**. *Toxicol Mech Methods*. 24(1):31–36, 2014.

SANKHLA MS, KUMAR R. **Fluoride Contamination of Water in India and its Impact on Public Health**. *ARC Journal of Forensic Science*, Vol 3, 2, pp 10-15, 2018.

SHUHUA, X.; ZIYOU, L.; LING, Y.; FEI, W.; SUN, G. **A role of fluoride on free radical generation and oxidative stress in BV-2 microglia cells.** Mediators of inflammation 2012, 102954, 2012.

TEN CATE JM & BUZALAF MAR. **Fluoride Mode of Action: Once There Was an Observant Dentist . . .** *J Dent Res*. 2019;98(7):725-730.

UNDE, M. P., PATIL, R. U., & DASTOOR, P. P. **The Untold Story of Fluoridation: Revisiting the Changing Perspectives.** *Indian journal of occupational and environmental medicine*, *22*(3), 121–127, 2018.

YAN, NLIU Y, LIU S, CAO S, WANG F, WANG Z, XI S. **Fluoride-Induced Neuron Apoptosis and Expressions Of Inflammatory Factors By Activating Microglia In Rats *Brain.*** *Mol Neurobiol*, 53(7):4449–4460, 2016.

YANG, L.; JIN, P.; WANG, X.; ZHOU, Q.; LIN, X.; XI, S. **Fluoride activates microglia, secretes inflammatory factors and influences synaptic neuron plasticity in the hippocampus of rats.** NeuroToxicology, 69, 108-120, 2018.

ANEXO A – CERTIFICADO DO COMITÊ DE ÉTICA EM EXPERIMENTAÇÃO ANIMAL

UFPA
Universidade Federal do Pará

Comissão de Ética no
Uso de Animais

CERTIFICADO

Certificamos que a proposta intitulada "INVESTIGAÇÃO DOS EFEITOS TOXICOLÓGICOS DA EXPOSIÇÃO CRÔNICA AO FLUORETO DE SÓDIO NO SISTEMA NEROVOSO CENTRAL DE CAMUNDONGOS", protocolada sob o CEUA nº 2422071217 (ID 000737), sob a responsabilidade de **Rafael Rodrigues Lima** *e equipe; Leonardo de Oliveira Bittencourt; Giza Hellen Nonato Miranda; Géssica de Oliveira Lopes; Lodinikki Lemoy Davis* - que envolve a produção, manutenção e/ou utilização de animais pertencentes ao filo Chordata, subfilo Vertebrata (exceto o homem), para fins de pesquisa científica ou ensino - está de acordo com os preceitos da Lei 11.794 de 8 de outubro de 2008, com o Decreto 6.899 de 15 de julho de 2009, bem como com as normas editadas pelo Conselho Nacional de Controle da Experimentação Animal (CONCEA), e foi **aprovada** pela Comissão de Ética no Uso de Animais da Universidade Federal do Pará (CEUA/UFPA) na reunião de 22/02/2018.

We certify that the proposal "Toxicological effects evaluation of chronic Sodium Fluoride exposure on Central Nervous System of mice", utilizing 60 Heterogenics mice (60 males), protocol number CEUA 2422071217 (ID 000737), under the responsibility of **Rafael Rodrigues Lima** *and team; Leonardo de Oliveira Bittencourt; Giza Hellen Nonato Miranda; Géssica de Oliveira Lopes; Lodinikki Lemoy Davis* - which involves the production, maintenance and/or use of animals belonging to the phylum Chordata, subphylum Vertebrata (except human beings), for scientific research purposes or teaching - is in accordance with Law 11.794 of October 8, 2008, Decree 6899 of July 15, 2009, as well as with the rules issued by the National Council for Control of Animal Experimentation (CONCEA), and was **approved** by the Ethic Committee on Animal Use of the Federal University of Para (CEUA/UFPA) in the meeting of 02/22/2018.

Finalidade da Proposta: Pesquisa

Vigência da Proposta: de 02/2018 a 09/2019 Área: Instituto de Ciências Biológicas

Origem:	Biotério Central ICB/UFPA						
Espécie:	Camundongos heterogênicos	sexo:	Machos	idade:	21 a 30 dias	N:	60
Linhagem:	Mus musculus			Peso:	30 a 40 g		

Local do experimento: Laboratório de Biologia Estrutural e Funcional - ICB

Belém, 04 de novembro de 2021

Barbarella de Matos Macchi
Profa. Dra. Barbarella de Matos Macchi
Coordenadora da Comissão de Ética no Uso de Animais
Universidade Federal do Pará

Mª Vivina B. Monteiro
Profa. Dra. Maria Vivina Barros Monteiro
Vice-Coordenadora da Comissão de Ética no Uso de Animais
Universidade Federal do Pará